In summary, the present study shows that ERRα is a novel adipogenic marker involved in the regulation of the expression of differentiation-related genes. These findings would have physiological relevance that ERRα can be potentially used as a molecular target for the treatment of obesity-related diseases.

Acknowledgments

We thank for Dr. T. Katagiri (Saitama Medical University) for technical advice. We are also grateful to T. Hishinuma, K. Chida and W. Satoh for their technical assistance. This work was supported in part by Grants-in-Aid from the Ministry of Health, Labor and Welfare; from the Japan Society for the Promotion of Science; from The Promotion and Mutual Aid Corporation for Private Schools of Japan. This work was supported in part by Grants of the Genome Network Project and the DECODE from the Ministry of Education, Culture, Sports, Science and Technology of Japan.

References

[1] Y. Shi, P. Burn, Lipid metabolic enzymes: emerging drug targets for the treatment of obesity, Nat. Rev. Drug Discov. 3 (2004) 695–710.
[2] E.E. Kershaw, J.S. Flier, Adipose tissue as an endocrine organ, J. Clin. Endocrinol. Metab. 89 (2004) 2548–2556.
[3] V. Giguère, N. Yang, P. Segui, R.M. Evans, Identification of a new class of steroid hormone receptors, Nature 331 (1988) 91–94.
[4] D.J. Heard, P.L. Norby, J. Holloway, H. Vissing, Human ERR, a third member of the estrogen receptor-related receptor (ERR) subfamily of orphan nuclear receptors: tissue-specific isoforms are expressed during development and in the adult, Mol. Endocrinol. 14 (2000) 382–392.
[5] H. Hong, L. Yang, M.R. Stallcup, Hormone-independent transcriptional activation and coactivator binding by novel orphan nuclear receptor ERR3, J. Biol. Chem. 274 (1999) 22618–22626.
[6] R. Sladek, J.A. Bader, V. Giguere, The orphan nuclear receptor estrogen-related receptor α is a transcriptional regulator of the human medium-chain acyl coenzyme A dehydrogenase gene, Mol. Cell. Biol. 17 (1997) 5400–5409.
[7] J. Luo, R. Sladek, J. Carrier, J.A. Bader, D. Richard, V. Giguere, Reduced fat mass in mice lacking orphan nuclear receptor estrogen-related receptor α, Mol. Cell. Biol. 23 (2003) 7947–7956.
[8] J.M. Huss, R.P. Kopp, D.P. Kelly, Peroxisome proliferator-activated receptor coactivator-1α (PGC-1α) coactivates the cardiac-enriched nuclear receptors estrogen-related receptor-α and -γ. Identification of novel leucine-rich interaction motif within PGC-1α, J. Biol. Chem. 277 (2002) 40265–40274.
[9] Y. Kamei, H. Ohizumi, Y. Fujitani, T. Nemoto, T. Tanaka, N. Takahashi, T. Kawada, M. Miyoshi, O. Ezaki, A. Kakizuka, PPARγ coactivator 1β/ERR ligand 1 is an ERR protein ligand, whose expression induces a high-energy expenditure and antagonizes obesity, Proc. Natl. Acad. Sci. USA 100 (2003) 12378–12383.
[10] D. Knutti, A. Kralli, PGC-1, a versatile coactivator, Trends Endocrinol. Metab. 12 (2001) 360–365.
[11] Z. Wu, P. Puigserver, U. Andersson, C. Zhang, G. Adelmant, V. Mootha, A. Troy, S. Cinti, B. Lowell, R.C. Scarpulla, B.M. Spiegelman, Mechanisms controlling mitochondrial biogenesis and respiration through the thermogenic coactivator PGC-1, Cell 98 (1999) 115–124.
[12] K. Yagi, D. Kondo, Y. Okazaki, K. Kano, A novel preadipocyte cell line established from mouse adult mature adipocytes, Biochem. Biophys. Res. Commun. 321 (2004) 967–974.
[13] K. Horie-Inoue, K. Takayama, H.U. Bono, Y. Ouchi, Y. Okazaki, S. Inoue, Identification of novel steroid target genes through the combination of bioinformatics and functional analysis of hormone response elements, Biochem. Biophys. Res. Commun. 339 (2006) 99–106.
[14] H. Niwa, K. Yamamura, J. Miyazaki, Efficient selection for high-expression transfectants with a novel eukaryotic vector, Gene 108 (1991) 193–199.
[15] H. Green, M. Meuth, An established pre-adipose cell line and its differentiation in culture, Cell 3 (1974) 127–133.
[16] A.K. Student, R.Y. Hsu, M.D. Lane, Induction of fatty acid synthetase synthesis in differentiating 3T3-L1 preadipocytes, J. Biol. Chem. 255 (1980) 4745–4750.
[17] S.M. Taylor, P.A. Jones, Multiple new phenotypes induced in 10T1/2 and 3T3 cells treated with 5-azacytidine, Cell 17 (1979) 771–779.
[18] T. Katagiri, A. Yamaguchi, T. Ikeda, S. Yoshiki, J.M. Wozney, V. Rosen, E.A. Wang, H. Tanaka, S. Omura, T. Suda, The non-osteogenic mouse pluripotent cell line, C3H10T1/2, is induced to differentiate into osteoblastic cells by recombinant human bone morphogenetic protein-2, Biochem. Biophys. Res. Commun. 172 (1990) 295–299.
[19] E.D. Rosen, B.M. Spiegelman, Molecular regulation of adipogenesis, Annu. Rev. Cell Dev. Biol. 16 (2000) 145–171.
[20] V.K. Mootha, C. Handschin, D. Arlow, X. Xie, J. St Pierre, S. Sihag, W. Yang, D. Altshuler, P. Puigserver, N. Patterson, P.J. Willy, I.G. Schulman, R.A. Heyman, E.S. Lander, B.M. Spiegelman, Errα and Gabpa/b specify PGC-1α-dependent oxidative phosphorylation gene expression that is altered in diabetic muscle, Proc. Natl. Acad. Sci. USA 101 (2004) 6570–6575.
[21] J.M. Huss, I.P. Torra, B. Staels, V. Giguere, D.P. Kelly, Estrogen-related receptor α directs peroxisome proliferator-activated receptor α signaling in the transcriptional control of energy metabolism in cardiac and skeletal muscle, Mol. Cell. Biol. 24 (2004) 9079–9091.
[22] S.N. Schreiber, R. Emter, M.B. Hock, D. Knutti, J. Cardenas, M. Podvinec, E.J. Oakeley, A. Kralli, The estrogen-related receptor α (ERRα) functions in PPARγ coactivator 1α (PGC-1α)-induced mitochondrial biogenesis, Proc. Natl. Acad. Sci. USA 101 (2004) 6472–6477.
[23] P. Puigserver, Z. Wu, C.W. Park, R. Graves, M. Wright, B.M. Spiegelman, A cold-inducible coactivator of nuclear receptors linked to adaptive thermogenesis, Cell 92 (1998) 829–839.
[24] J. Lin, P.H. Wu, P.T. Tarr, K.S. Lindenberg, J. St-Pierre, C.Y. Zhang, V.K. Mootha, S. Jager, C.R. Vianna, R.M. Reznick, L. Cui, M. Manieri, M.X. Donovan, Z. Wu, M.P. Cooper, M.C. Fan, L.M. Rohas, A.M. Zavacki, S. Cinti, G.I. Shulman, B.B. Lowell, D. Krainc, B.M. Spiegelman, Defects in adaptive energy metabolism with CNS-linked hyperactivity in PGC-1α null mice, Cell 119 (2004) 121–135.
[25] J.A. Villena, M.B. Hock, W.Y. Chang, J.E. Barcas, V. Giguere, A. Kralli, Orphan nuclear receptor estrogen-related receptor α is essential for adaptive thermogenesis, Proc. Natl. Acad. Sci. USA 104 (2007) 1418–1423.
[26] J. Lin, P.T. Tarr, R. Yang, J. Rhee, P. Puigserver, C.B. Newgard, B.M. Spiegelman, PGC-1β in the regulation of hepatic glucose and energy metabolism, J. Biol. Chem. 278 (2003) 30843–30848.
[27] J. St-Pierre, J. Lin, S. Krauss, P.T. Tarr, R. Yang, C.B. Newgard, B.M. Spiegelman, Bioenergetic analysis of peroxisome proliferator-activated receptor γ coactivators 1α and 1β (PGC-1α and PGC-1β) in muscle cells, J. Biol. Chem. 278 (2003) 26597–26603.
[28] D. Nichol, M. Christian, J.H. Steel, R. White, M.G. Parker, RIP140 expression is stimulated by estrogen-related receptor α during adipogenesis, J. Biol. Chem. 281 (2006) 32140–32147.
[29] G. Leonardsson, J.H. Steel, M. Christian, V. Pocock, S. Milligan, J. Bell, P.W. So, G. Medina-Gomez, A. Vidal-Puig, R. White, M.G. Parker, Nuclear receptor corepressor RIP140 regulates fat accumulation, Proc. Natl. Acad. Sci. USA 101 (2004) 8437–8442.

Cytochrome P450 2B6 is a Growth-Inhibitory and Prognostic Factor for Prostate Cancer

Jinpei Kumagai,[1] Tetsuya Fujimura,[1] Satoru Takahashi,[1]* Tomohiko Urano,[2] Tetsuo Ogushi,[1] Kuniko Horie-Inoue,[3] Yasuyoshi Ouchi,[2] Tadaichi Kitamura,[1] Masami Muramatsu,[3] Bruce Blumberg,[4] and Satoshi Inoue[2,3]

[1]*Department of Urology, The University of Tokyo, Hongo, Bunkyo-ku, Tokyo, Japan*
[2]*Department of Geriatric Medicine, Faculty of Medicine, The University of Tokyo, Hongo, Bunkyo-ku, Tokyo, Japan*
[3]*Research Center for Genomic Medicine, Saitama Medical University, Yamane, Hidaka-shi, Saitama, Japan*
[4]*Department of Developmental and Cell Biology, University of California, Irvine, California*

BACKGROUND. Cytochrome P450s (CYPs) influence the biological effects of carcinogens, drugs and hormones including testosterones. Among them, Cytochrome P450 2B6 (CYP2B6) plays a critical role in the deactivation of testosterone. In the present study, we examined CYP2B6 expression in human prostate tissues and prostate cancer.

METHODS. Immunohistochemical analysis was performed in 98 benign and 106 malignant prostate tissues and patients' charts were reviewed for clinical, pathologic and survival data. We also investigated whether stable expression of CYP2B6 in LNCaP (human prostate cancer cell line) influences cellular proliferation.

RESULTS. CYP2B6 was abundantly expressed in the normal epithelial cells compared to the prostate cancer cells. Significant immunostaining of CYP2B6 was found in 75 of 106 samples (71%), in the cytoplasm of cancerous tissue samples. CYP2B6 immunoreactivity was inversely correlated with high Gleason score ($P < 0.001$). Decreased immunoreactivity of CYP2B6 significantly correlated with poor prognosis ($P < 0.0001$). Univariate and multivariate hazard analyses revealed a significant correlation of decreased CYP2B6 expression with poor cancer-specific survival ($P = 0.0028$ and 0.0142, respectively). Furthermore, overexpression of CYP2B6 in LNCaP cells significantly decreased testosterone-induced proliferation.

CONCLUSIONS. These results demonstrated that decreased expression of CYP2B6 might play a role in the development of prostate cancer, and be useful as the prognostic predictor for human prostate cancer. *Prostate 67: 1029–1037, 2007.* © 2007 Wiley-Liss, Inc.

KEY WORDS: **testosterone; proliferation and prognosis**

INTRODUCTION

Prostate cancer is one of the most common malignancies in the world. There is abundant evidence that androgens influence the development and progression of prostate cancer [1–3]. Since most of prostate cancer is androgen-dependent, standard treatment for metastatic prostate cancer patients is androgen deprivation therapy (ADT). However the beneficial effects of ADT are transient and prostate cancer progresses to recurrent cancer. Recent reports showed that levels of testosterone and its metabolites, dihydrotestosterone (DHT) and androstenediol, were still sufficiently high to activate the androgen receptor in recurrent prostate

Abbreviations: ADT, androgen deprivation therapy; CYPs, Cytochrome P450s; DHT, dihydrotestosterone; GS, Gleason score; IR, immunoreactivity; PSA, prostate-specific antigen.

Grant sponsor: Ministry of Health, Labour and Welfare; Grant sponsor: Japan Society for the Promotion of Science; Grant sponsor: Genome Network Project; Grant sponsor: Ministry of Education, Culture, Sports, Science and Technology; Grant sponsor: Promotion and Mutual Aid Corporation for Private Schools.

*Correspondence to: Satoru Takahashi, MD, Department of Urology, Faculty of Medicine, The University of Tokyo, 7-3-1 Hongo, Bunkyo-ku, Tokyo 113-8655, Japan. E-mail: tsatoru@med.nihon-u.ac.jp

Received 2 November 2006; Accepted 7 March 2007
DOI 10.1002/pros.20597
Published online 23 April 2007 in Wiley InterScience (www.interscience.wiley.com).

cancer during ADT [4,5]. The presence of testosterone and its metabolites in recurrent prostate cancer is likely to be significant in prostate cancer progression.

Cytochrome P450s (CYPs) play an important role in biotransformation of xenobiotics such as pharmaceutical drug, environmental contaminants. In addition, these enzymes metabolize endogenous compounds such as steroid hormones [6]. In the liver CYP2B6 hydroxylates testosterone, which results in the deactivation of the hormonal function. It also metabolizes drugs including anti-cancer prodrugs [7]. CYPs have also been detected in extrahepatic tissues, such as the intestine, lung, kidney and brain [8], and breast cancer tissues [9–11]. It was reported that CYP bioactivates anti-cancer prodrug ifosfamide [9] in breast cancers and that the expression of CYPs including CYP2B6 was lower in the tumor tissue than in the adjacent normal tissue [10,11]. The prostate expresses several enzymes involved in androgen metabolism. Since androgens are substrates for multiple CYPs (e.g., CYP2B6, CYP3A4) we undertook to study the expression of this enzyme family in prostate tissues. There are some data from RT-PCR analysis concerning the expression of CYP1A1, CYP1A2, CYP1B1, CYP2B6, and CYP3A4 in human prostate [12,13]. However the expression of CYPs has not been well studied in benign prostate tissues and prostate cancer at the protein level. Since hepatic CYP2B6 is important in testosterone deactivation, we investigated its expression in human prostate tissues using immunohistochemistry. We examined the potential clinical significance of this expression and the influence of CYP2B6 overexpression on the proliferation of the LNCaP cells.

MATERIALS AND METHODS

Antibody and Expression Plasmid Constructs

An anti-CYP2B6 rabbit polyclonal antibody was purchased from Research Diagnostics, Inc. (Flanders, NJ); anti-FLAG M2 antibody and anti-β-actin antibody was from Sigma (St. Louis, MO); and anti-rabbit IgG Alexa Fluor 594 and anti-mouse IgG Alexa Fluor 488 were from Molecular Probes (Invitrogen, Carlsbad, CA). The cDNA encoding amino-terminal FLAG-tagged human CYP2B6 was amplified from the IMAGE-clone, NIH MGC 195 (Open Biosystems), subcloned into a mammalian expression vector pcDNA3 (Invitrogen) and the resulting FLAG-tagged CYP2B6 expression plasmid (pcDNA3-CYP2B6-FLAG) was verified by DNA sequencing.

Cell Culture and Transfection

COS7 cells were cultured in Dulbecco's modified Eagle's medium (DMEM) containing 10% FBS. LNCaP (Human prostate cancer cell line) was purchased from American Type Culture Collection (Manassas, VA). LNCaP was maintained in RPMI1640 media supplemented with 2 mM glutamine, 1% nonessential amino acids, 100 U/ml streptomycin/penicillin and 10% fetal calf serum (FCS). Transfection was performed by using FuGENE6 (Roche, Indianapolis, IN) according to the manufacturer's instruction.

Immunofluorescence Staining

Cells were grown on 12-mm circle cover glasses (Fisher) in 24-well plates. After 16 hr, living cells were washed three times with phosphate-buffered saline (PBS), fixed with 4% paraformaldehyde/0.1 M phosphate buffer for 5 min at room temperature, washed once with PBS, and permeabilized with 0.2% Triton-X 100 in PBS for 10 min. After another washing step with PBS and blocking in 3% bovine serum albumin (BSA)/TBST (100 mM Tris–HCl pH 8.0, 150 mM NaCl, 0.05% Tween 20) for 30 min, cells were first incubated with rabbit anti-CYP2B6 antibody (1:200) and mouse anti-FLAG M2 antibody (1:500) in 3% BSA/TBST for 1 hr at room temperature, washed three times with PBS, subsequently incubated with anti-rabbit IgG Alexa Fluor 594 (1:2,000) and anti-mouse IgG Alexa Fluor 488 (1:2,000) in 3% BSA/TBST for 1 hr at room temperature. Nuclei were stained with DAPI (4′,6-diamidino-2-phenylindole). After cells were washed three times with PBS, cover glasses were mounted in 1.25% DABCO, 50% PBS, 50% glycerol and visualized using a digital microscope (VH-8000, Keyence, Japan).

Western Blot Analysis

Western blot analysis was performed using cellular protein extracts. Cells were rinsed twice with ice-cold PBS and lysed in 200 μl Nonidet P-40 lysis buffer (50 mM Tris–HCl [pH 7.4], 150 mM NaCl, 10 mM NaF, 5 mM EDTA, 5 mM EGTA, 2 mM sodium vanadate, 0.5% sodium deoxycholate, 1 mM dithiothreitol [DTT], 1 mM phenylmethylsulfonylfluoride [PMSF], 2 μg/ml aprotinin and 0.1% Nonidet P-40), and the lysates were cleared by centrifugation at 15,000*g* for 15 min at 4°C. Total protein lysate (20 μg) was fractionated on sodium dodecyl sulfate (SDS)-12.5% polyacrylamide gels, and electrophoretically transferred onto polyvinylidene difluoride (PVDF) membranes (Immobilon, Millipore Co., Bedford, MA).The membranes were blocked in Tris-buffered saline (TBS) with 5% skim milk for 30 min, then incubated with 5 ml each of 1:500 diluted anti-CYP2B6 antibody or 1:1,000 diluted anti-FLAG M2 antibody (Sigma) at room temperature for 3 hr. Each membrane was washed in TBS with 0.1% Tween 20 and incubated with 1:5,000 diluted horseradish peroxidase-conjugated donkey anti-rabbit immunoglobulin G

(Ig G) or 1:5,000 diluted horseradish peroxidase-conjugated sheep anti-mouse Ig G (Amersham Pharmacia Biothech, Arlington Heights, IL) at room temperature for 1 hr. Bands were visualized with the chemiluminescence-based ECL plus detection system (Amersham Pharmacia Biotech). The membranes were exposed to X-ray film. All experiments were performed a minimum of three times.

Tissue Selections and Patient Characteristics

Formalin-fixed, paraffin-embedded sections were obtained from 106 patients who underwent radical prostatectomy for prostatic adenocarcinoma between 1987 and 2001. We obtained informed consent from all the patients. The age of the patients ranged from 52 to 78 years (mean 66.8 ± 6.0), and pretreatment serum PSA (prostate-specific antigen) level ranged from 2.2 to 136 ng/ml (mean 16.9 ± 19.5). The pathological stages included B ($n = 33$), C ($n = 59$) and D_1 ($n = 14$). Prostatic tissue sections submitted for this study contained 98 benign and 106 cancerous foci. The cancerous lesions consisted of tumors with Gleason score (GS) 6 ($n = 22$), 7 ($n = 41$), 8 ($n = 20$), 9 ($n = 22$), and 10 ($n = 1$), which was evaluated by two trained pathologists. Thirty-five patients (33%) were treated with surgery alone, whereas the remaining patients received adjuvant anti-androgen therapy. Patients were followed post-operatively by their surgeons at 3-month intervals to 5 years and yearly thereafter. Mean patient follow-up period was 82 ± 39 months (range 10–192). During the follow-up period, 77 patients (73%) are alive with no evidence of the disease and 12 (11%) are alive with biochemical or clinical recurrence. Eleven patients (10%) died from prostate cancer and 6 (6%) died from other diseases during the follow-up period.

Immunohistochemistry

Immunohistochemical analysis was performed employing the streptavidin–biotin amplification method using a peroxidase catalyzed signal amplification system: CSA system (DAKO, Carpinteria, CA) as previously described [14]. CSA was used following the manufacturer-supplied protocol. Six μm tissue-sections were deparaffinized, rehydrated through a graded ethanol series, and rinsed in PBS. For antigen retrieval, the sections were autoclaved at 120°C for 15 min in citric acid buffer (2 mM citric acid and 9 mM trisodium citrate dehydrate, pH 6.0). After blocking endogenous peroxidase with 0.3% H_2O_2, the sections were incubated in 10% bovine serum for 10 min. Application of the polyclonal antibody for CYP2B6 (1:200 dilution) was followed by sequential 15-min incubations with biotinylated link antibody, streptavidin–biotin–peroxidase complex, amplification reagent, and streptavidin-peroxidase. The antigen-antibody complex was visualized with 3,3′-diaminobenzidine (DAB) solution (1 mM DAB, 50 mM Tris–HCl buffer pH 7.6, and 0.006% H_2O_2). For negative controls, normal rabbit IgG was used instead of the primary antibodies. As positive controls, sections of human normal liver were immunoassayed with the primary antibodies in the same manner as described above.

Immunohistochemical Assessment

Immunostained slides were evaluated for the proportion (0, none; 1, <1/100; 2, 1/100 to 1/10; 3, 1/10 to 1/3; 4, 1/3 to 2/3; 5, >2/3) and the intensity (0, none; 1, weak; 2, moderate; 3, strong) of positively stained cells [15]. The total scores of immunoreactivity (0–8) were obtained as the sum of the proportion and the intensity. For immunohistochemical assessment, two investigators (TF and JK) evaluated the tissue sections independently. If the IR score (immunoreactivity score) differed between the two investigators, a third investigator (ST) evaluated the samples an average IR score was adopted. Since almost all bénign foci showed >5 of IR scores for CYP2B6, we defined IR score 5 as a cutoff for positive immunoreactivity of CYP2B6.

Generation of LNCaP Stably Expressing CYP2B6-FLAG

LNCaP was transfected with an expression vector, pcDNA3-CYP2B6-FLAG or vector alone using FuGENE6. G418 resistant cells were selected and several independent clones were isolated.

3-(4,5-Dimethylthiazol-2-yl)-5-(3-Carboxymethoxyphenyl-2-(4-Sulfophenyl)-2H-Tetrazolium (MTS) Assay

Cell growth rate was measured using a MTS proliferation assay (Cell Titer 96 AQueous One Solution Cell Proliferation Assay, Promega, Madison, WI). The assay was performed according to manufacturer's instructions. Five thousand cells were seeded in 96-well plates and cultured in RPMI supplemented with 10% FBS for 48 and 72 hr. Before testing, 10 μl of MTS reagent was added and the cells were incubated for a further 4 hr at 37°C. The optical density (OD) was measured at a wavelength of 490 nm by a microplate reader (Bio-Rad model 550, Japan). Each time point was performed in quadruplicate wells and each experiment was repeated at least three times. To evaluate effects of testosterone on the growth of LNCaP-CYP2B6-FLAG or LNCaP-Vector clones, the cells were cultured in phenol-red free medium with 10% charcoal-stripped FBS for 48 hr

before experiments. Then 5,000 cells were seeded in 96-well plates and cultured with either vehicle control or testosterone at a dose of 10^{-10} or 10^{-8} M for 48 hr. Percent increase of OD compared with vehicle control was calculated.

Statistical Analysis

Correlations between IR score and clinicopathological characteristics (age, pretreatment serum PSA level, pathological stage and GS) were evaluated using the Student's *t*-test or chi-square test. Cancer-specific survival curves were obtained by the Kaplan–Meier method and verified by the log rank (Mantel-Cox) test. The comparisons between OD of LNCaP clones were evaluated using the Student's *t*-test. Statistical assessment was analyzed by Stat View-J 5.0 software (SAS Institute, Cary, NC) and *P* values less than 0.05 were regarded as statistically significant.

RESULTS

Immunofluorescence Staining of Transfected COS7 Cells

We transiently transfected COS7 cells using pcDNA3-CYP2B6-FLAG and immunostained with anti-CYP2B6 and anti-FLAG M2 antibodies. The anti-CYP2B6 antibody revealed a cytoplasmic staining pattern in CYP2B6-FLAG overexpressed COS7. This expression pattern was shared with the anti-FLAG antibody (Fig. 1A), demonstrating that the protein was located in the cytoplasm.

Validation of CYP2B6 Antibody by Western Blot Analysis

We next transiently transfected COS7 cells using CYP2B6-FLAG expression plasmid for Western blot analysis. As expected, the CYP2B6 antibody detected a 53-kDa band in pCDNA3-CYP2B6-FLAG transfected COS7. A band of apparently the same size was detected by the FLAG M2 antibody (Fig. 1B arrow head).

Immunohistochemistry

Diffuse, but intense CYP2B6 immunostaining was detected in the cytoplasm of benign prostate epithelium. In contrast, immunoreactivity of CYP2B6 was low in the cancer cells. In addition, immunoreactivity of high GS prostate cancer was markedly less than low GS prostate cancer (Fig. 2). The results for the expression of CYP2B6 in the human prostate tissues are shown in Figure 3. When an IR score ≥ 5 was defined as positive, positive CYP2B6 immunoreactivity was identified in 96 (98.0%) benign prostate epithelium cases. Among the 63 low GS prostate cancer cases, positive CYP2B6 immunoreactivity (IR score ≥ 5) was observed in 55 cases (87.3%). Of the 43 high GS prostate cancer cases, positive CYP2B6 immunoreactivity was observed in 20 cases (46.5%). Therefore, a strong association exists between high GS prostate cancer and low CYP2B6 immunoreactivity.

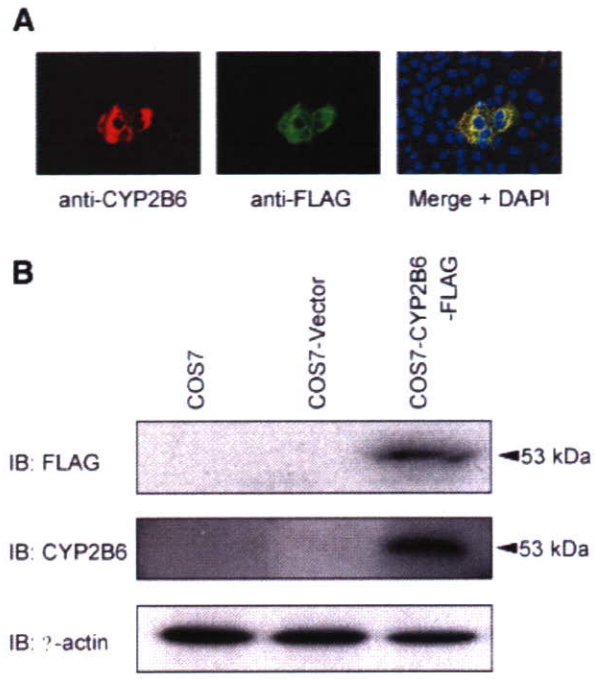

Fig. 1. Immunofluorescence staining of transfected COS7 cells and validation of CYP2B6 antibody by Western blot analysis. A: COS7 cells were grown on cover glasses, transiently transfected with CYP2B6-FLAG expression plasmid, fixed with paraformaldehyde and stained with anti-CYP2B6 antibody and anti-FLAG antibody. Nuclei were counterstained with DAPI. Signals from CYP2B6 (left panel) and signals from FLAG (middle panel) antibody shared an identical subcellular distribution. Merged images are shown on the right panel. Scale bars, 20 μm. B: Cell extracts from untransfected, pcDNA3 empty plasmid transfected, and pcDNA3-CYP2B6-FLAG transfected COS7 cells were resolved by SDS-PAGE and transferred to PVDF membrane. Blot was probed with the anti-CYP2B6 polyclonal antibody (1:500), anti-FLAG antibody (1:1,000) and anti-β-actin antibody (1:1,000). CYP2B6 antibody detected a 53-kDa band in pcDNA3-CYP2B6-FLAG transfected COS7 cells, which was coincided with a band detected by anti-FLAG antibody.

Correlation of CYP2B6 Expression With Clinicopathological Characteristics in Prostate Cancer

This association between CYP2B6 and GS, led us to evaluate the potential correlation between CYP2B6 immunoreactivity and clinicopathological characteristics. Age, pretreatment serum PSA level, GS and pathologic stage) were evaluated (Table I). CYP2B6 immunoreactivity was significantly lower in high GS

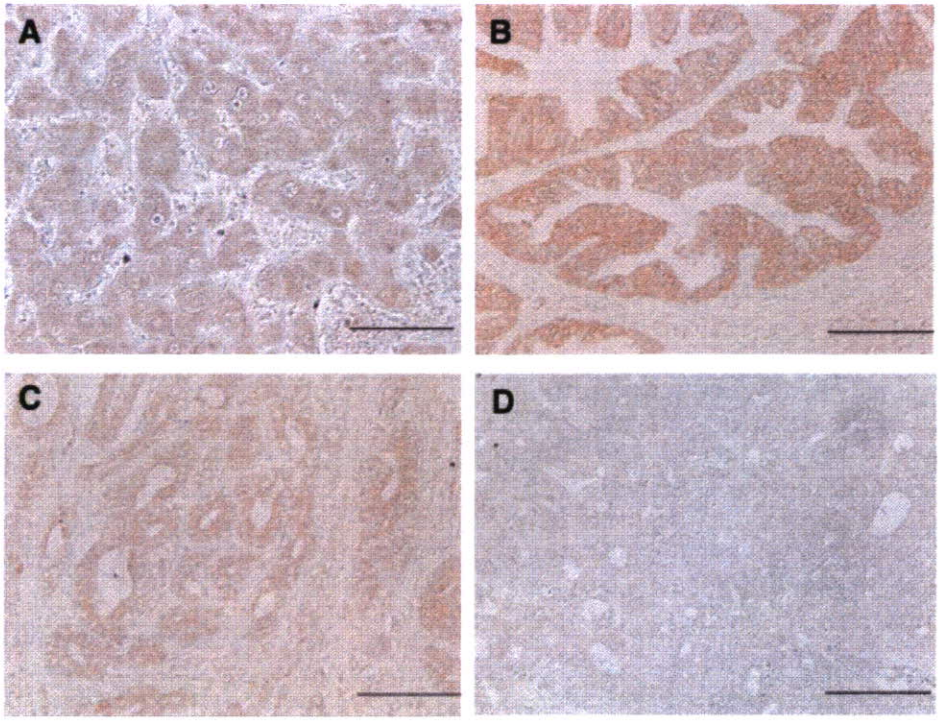

Fig. 2. Expression of CYP2B6 in human liver and benign prostate tissue, low GS and high GS prostate cancer. **A**: Strong staining (intensity: 3) of CYP2B6 was identified in liver. **B**: Strong staining (intensity: 3) of CYP2B6 was identified in benign epithelium. **C**: Moderate immunoreactivity (intensity: 2) was identified in low GS prostate cancer (GS 6). **D**: Weak immunoreactivity of CYP2B6 (intensity: 1) was observed in high GS prostate cancer (GS 9). Scale bars, 100 μm.

cancer (GS 8–10) than in low GS cancer (GS 2–7) ($P < 0.001$).

Figure 4 shows a cancer-specific survival curve prepared by the Kaplan–Meier method. Fifteen of 31 (48.4%) CYP2B6-negative cases had died from prostate cancer during the follow-up period. Patients with CYP2B6-negative prostate cancer had significantly worse cancer-specific survival than those with CYP2B6-positive prostate cancer ($P < 0.0001$, log rank test). Table II shows the prognostic value of PSA, pathological stage, GS and CYP2B6 immunoreactivity in univariate and multivariate proportional analyses for cancer-specific survival. In univariate analyses, CYP2B6 immunoreactivity was significantly ($P = 0.003$) related to cancer specific survival as well as the GS ($P = 0.014$) and pathological stage ($P = 0.035$). In multivariate analysis, among four parameters, only CYP2B6 immunoreactivity retained independent prognostic significance ($P = 0.014$). The relative risk for cancer specific mortality was 14.0 (95% CI 1.69–115.4) for patients with CYP2B6-negative prostate cancer.

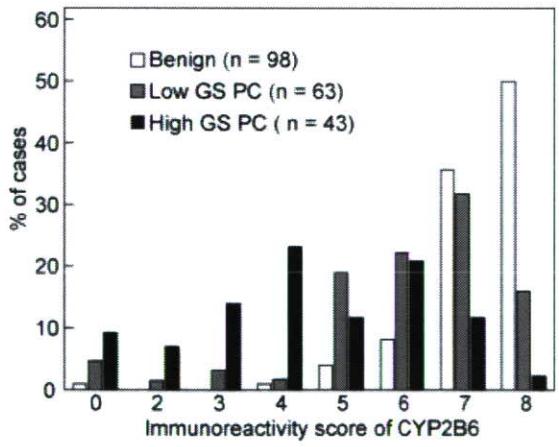

Fig. 3. Immunoreactivity score of CYP2B6 in human benign, low GS prostate cancer and high GS prostate cancer. Positive immunostaining (IR score ≥5) was observed more frequently in benign prostate than prostate cancer tissue and more frequently in low GS prostate cancer than in high GS prostate cancer.

Generation of LNCaP Stably Expressing CYP2B6-FLAG

To explore whether constitutive CYP2B6 expression influences cancer cell proliferation in human prostate cancer cell line, we generated LNCaP stably expressing human CYP2B6-FLAG protein and LNCaP clones with the vector (LNCaP-Vector clone #1 and #4). We selected two LNCaP-CYP2B6-FLAG clones #2 and #3 that express CYP2B6-FLAG protein as confirmed by Western blotting using anti-FLAG M2 antibody (Fig. 5A). Further we confirmed protein expression of

TABLE I. Relationship Between Expression of CYP2B6 and the Clinicopathological Findings in PC (n = 106)

	Immunoreactivity of CYP2B6[a]		
	Negative (n = 31)	Positive (n = 75)	*P* value
Age	66.2 ± 5.6	66.9 ± 6.1	0.59
Serum PSA (ng/ml)	19.2 ± 19.3	13.7 ± 12.7	0.08
Gleason score			
2–7	8 (12.7)	55 (87.3)	**<0.001**
8–10	23 (53.5)	20 (46.5)	
Pathological stage			
B, C	24 (22.6)	68 (77.4)	0.07
D1	7 (50)	7 (50)	

[a]IR score 0–4 and 5–8 were defined as negative and positive immunoreactivity, respectively.

LNCaP-CYP2B6-FLAG stable clones by immunofluorescence staining (Fig. 5B). Almost all stable cells expressed CYP2B6-FLAG protein, and the immunoreactivity detected by the anti-FLAG antibody and anti-CYP2B6 antibody were indistinguishable.

MTS Proliferation Assay of LNCaP

Proliferation of LNCaP cells was determined by MTS assay. The proliferation of LNCaP-CYP2B6-FLAG stable clones was significantly reduced after 48 and 72 hr incubation compared to vector clones ($P < 0.0001$) (Fig. 5C). The result indicated that stable expression of CYP2B6 decreased the proliferation of cultured prostate cancer cells. This is consistent with the immunohistochemical results that showed decreased expression of CYP2B6 was associated with a poor prognosis.

Inhibitory Effect of CYP2B6 on Testosterone-Induced Growth

To determine whether effects of testosterone were inhibited by expression of CYP2B6, growth of LNCaP-CYP2B6-FLAG and LNCaP-Vector clones were assayed after testosterone treatment. MTS assay showed that the percent increase of OD was significantly decreased in LNCaP-CYP2B6-FLAG stable clones after 48 hr incubation at doses of 10^{-10} M ($P < 0.0001$) and 10^{-8} M ($P = 0.012$) of testosterone compared to vector clones (Fig. 5D). These data indicated that testosterone-induced growth was inhibited by CYP2B6 expression clearly.

DISCUSSION

In human liver, CYP2B6 ranges between 2 and 10% of the total P450 content [16]. Moreover, CYP2B6 is involved in the metabolism of nearly 25% of drugs on the market today [17]. CYPs expressed in the liver are well known to play pivotal roles in the metabolism of endobiotics, xenobiotic and pharmaceutical drugs. However, CYPs are also expressed in extra-hepatic tissues. Recent years have seen an increased interest in investigation into the presence, function and regulation of CYPs in such tissues, particularly in tumors. CYP1B1 is reported to be overexpressed in human prostate cancer and it was postulated that it contributes to the

TABLE II. Univariate and Multivariate Proportional Hazard Analyses of Cancer-Specific Survival (n = 106)

	Univariate			Multivariate		
Variable	Hazard ratio	95% index	*P* value	Hazard ratio	95% index	*P* value
PSA (>10 vs. ≤10)	0.79	0.23–2.8	0.73	0.75	0.17–3.26	0.69
Gleason score (high vs. low[a])	13.4	1.71–105.2	**0.014**	5.46	0.61–49.6	0.13
Pathological stage (D1 vs. B, C)	3.8	1.01–12.9	**0.035**	2.02	0.47–8.2	0.34
CYP2B6 (negative vs. positive[b])	23.1	2.94–181.5	**0.0028**	14	1.69–115.4	**0.014**

[a]High Gleason score: 8–10, low: 2–7.
[b]IR score 0–4 and 5–8 were defined as negative and positive immunoreactivity, respectively.

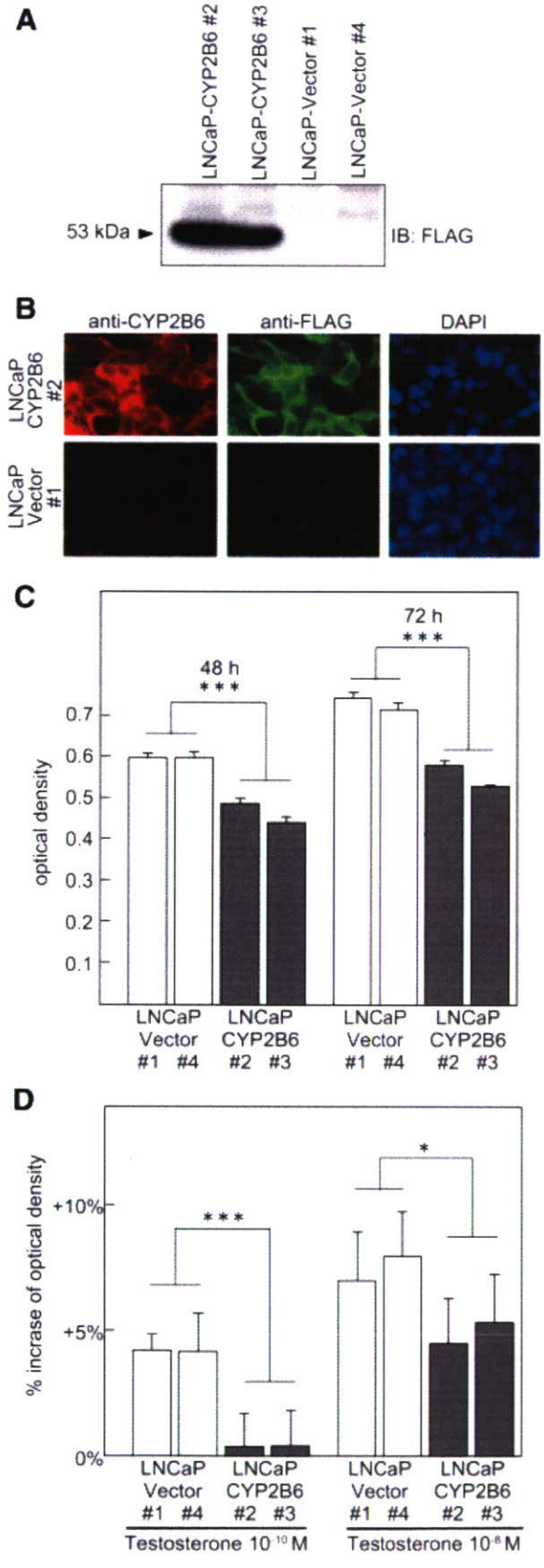

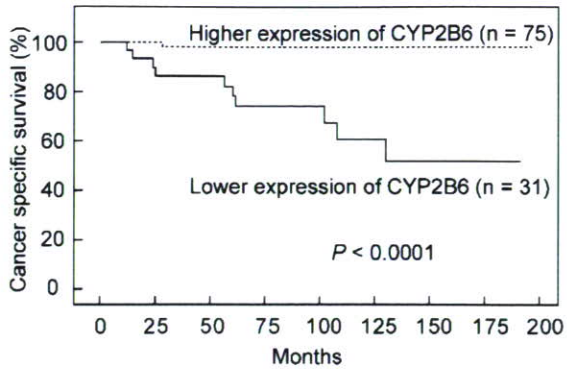

Fig. 4. Cancer-specific survival in 106 prostatic cancer patients relative to the immunoreactivity of CYP2B6. Cancer-specific survival of 31 patients with negative CYP2B6 expression (IR score <5) was significantly worse than that of 75 positive expression cases (IR score ≥ 5) ($P < 0.001$).

development or progression of prostate cancer by activating pro-carcinogens [18]. A few reports are available on the expression of CYP2B6 mRNA in prostate [13]. Despite the important role of CYP2B6 in hepatic deactivation of testosterone, extra-hepatic expression of CYP2B6 protein has not been extensively studied, particularly in prostate cancer. Therefore, we studied the expression of CYP2B6 in human prostate tissues using immunohistochemistry and evaluated its clinical significance.

In the present study, we demonstrated CYP2B6 expression in human benign and malignant tissues by immunohistochemical analyses. CYP2B6 immunoreactivity was low in prostate cancer cells, whereas intense and diffuse CYP2B6 immunoreactivity was found in the normal or hyperplastic prostate epithelium. In univariate analysis, CYP2B6 immunoreactivity, GS and pathological stage were significantly related to cancer specific survival, but pretreatment PSA was not associated with cancer-specific survival. Pretreatment serum PSA level is generally an established prognostic

Fig. 5. Overexpression of CYP2B6 decreases growth of LNCaP cells. **A**: Western blot analysis of LNCaP stably expressing CYP2B6-FLAG (LNCaP-CYP2B6-FLAG) or empty vector (LNCaP-Vector). CYP2B6-FLAG protein was overexpressed in LNCaP-CYP2B6-FLAG clones. LNCaP-Vector clones were used for control. **B**: Immunofluorescence staining of LNCaP. Almost all cells expressed CYP2B6-FLAG protein in LNCaP-CYP2B6-FLAG clone #2 (upper panel). CYP2B6 immunoreactivity was not detected in LNCaP-Vecter cells as shown in lower panel. **C**: Proliferation of LNCaP stable clones was determined by MTS assay. Cell proliferation was evaluated after 48 and 72 hr incubation. ***$P < 0.0001$, compared to vector controls. **D**: Proliferative effects of testosterone were determined by MTS assay. Percent increase of OD was significantly decreased in LNCaP-CYP2B6-FLAG stable clones after 48 hr incubation compared to vector clones at doses of 10^{-10} and 10^{-8} M testosterone. ***$P < 0.0001$, *$P < 0.05$, compared to vector controls.

factor for PSA recurrence, but not for cancer-specific survival after radical prostatectomy [19]. The restricted low range of preoperative PSA in the present study (25th and 75th percentile, 6.2 and 18.1) may have limited the predictive value of preoperative PSA levels on cancer-specific survival. Data reported by other groups were consistent with our results that only pT stage, and GS were significant prognostic factors about cancer specific survival after radical prostatectomy [19,20].

Expression of CYP2B6 has been recently investigated in a few carcinomas, including breast cancer and hepatocellular carcinoma (HCC). In breast cancer, CYP2B6 mRNA was down-regulated in the tumor tissue compared with normal adjacent tissue [10]. In addition, CYP2B6 mRNA was significantly lower in HCC with venous invasion than in HCC without venous invasion [21]. These findings suggest that CYP2B6 expression may be decreased in the development of cancers that are closely related to substrates of CYP2B6.

CYPs sensitize tumor xenograft to anticancer prodrugs such as cyclophosphamide (CPA). The anticancer activity of CPA in cultured tumor cells and in rodent and human xenograft models is substantially increased by introduction of cDNAs encoding CYP2B6, which are major catalysts of CPA activation in rat and human liver, respectively [22,23]. On the other hand Ikezoe et al. demonstrated that ritonavir blocked the docetaxel-induced expression of CYP3A4 at the mRNA level in prostate cancer DU145 cells and enhanced the antitumor effect of docetaxel in vitro and in BNX nude mice bearing DU145 tumors [24]. These findings showed that extrahepatic CYPs also biotransformed drugs like hepatic CYPs and that this biotransformation may be associated with activation or deactivation of anticancer drugs.

Testosterone is inactivated in the liver and the prostate. CYP2B6 are known to function in hepatic testosterone inactivation [7,25]. In the prostate, several enzymes are involved in the metabolism of testosterone. 5α-Reductase converts testosterone to DHT. DHT is converted by the enzymes 3α-and 3β-hydroxysteroid oxidoreductase into 5α-androstane-3α,17β-diol (3α-diol) and 5α-androstane-3β,17β-diol (3βA-diol), respectively. The 3βA-diol is further hydroxylated to 6α-, 6β-, 7α-, and 7β-triols which are inactive as androgens and excreted from the prostate. In addition, rat CYPs catalyze the 6α-, 6β-, 7α-, and 7β-hydroxylation of the 3βA-diol in the ventral prostate [26–28] However little is known about the role of CYPs in testosterone metabolism in human prostate. We hypothesized that, consistent with the role of CYP2B6 in liver and the role of CYPs in rat prostate, CYP2B6 might play an important role in testosterone metabolism in the human prostate. If so, then decreased expression of CYP2B6 might contribute to elevated DHT levels in the prostate, thus promoting cancer progression. Consistent with this hypothesis, our present study showed that decreased expression of CYP2B6 significantly correlated with poor prognosis in human prostate cancer. Moreover, stable overexpression of CYP2B6 in LNCaP reduced their proliferation as well as testosterone-induced proliferation. Taken together, these results support the view that CYP2B6 interferes with proliferation of prostate cancer cells by either catabolize some pro-proliferative substances such as testosterones, or metabolize anti-proliferative substances.

CONCLUSIONS

In conclusion, our results indicate that decreased CYP2B6 expression was an independent prognostic factor for prostate cancer and that CYP2B6 overexpression interfered with proliferation of LNCaP cells. Immunoreactivity of CYP2B6 may therefore be useful in selecting patients with more aggressive tumor for adjuvant therapy. These results suggest that CYP2B6 has significant anti-tumor effects in prostate cancer. Therefore, compounds which highly induce CYP2B6 such as phenobarbital, rifampicin, clotrimazole, phenytoin and carbamazepine [29–31] might be of clinical benefit in the treatment of recurrent prostate cancer.

ACKNOWLEDGMENTS

This work was supported in part by grants-in-aid from the Ministry of Health, Labor and Welfare and from the Japan Society for the Promotion of Science and by a grant of the Genome Network Project from the Ministry of Education, Culture, Sports, Science and Technology of Japan and for Development of New Technology from The Promotion and Mutual Aid Corporation for Private Schools of Japan.

REFERENCES

1. Hsing AW, Reichardt JK, Stanczyk FZ. Hormones and prostate cancer: Current perspectives and future directions. Prostate 2002;52(3):213–235.
2. Ross RK, Bernstein L, Lobo RA, Shimizu H, Stanczyk FZ, Pike MC, Henderson BE. 5-Alpha-reductase activity and risk of prostate cancer among Japanese and US white and black males. Lancet 1992;339(8798):887–889.
3. Giovannucci E, Stampfer MJ, Krithivas K, Brown M, Dahl D, Brufsky A, Talcott J, Hennekens CH, Kantoff PW. The, CAG repeat within the androgen receptor gene and its relationship to prostate cancer. Proc Natl Acad Sci USA 1997;94(7):3320–3323.
4. Mizokami A, Koh E, Fujita H, Maeda Y, Egawa M, Koshida K, Honma S, Keller ET, Namiki M. The adrenal androgen androstenediol is present in prostate cancer tissue after androgen deprivation therapy and activates mutated androgen receptor. Cancer Res 2004;64(2):765–771.

5. Titus MA, Schell MJ, Lih FB, Tomer KB, Mohler JL. Testosterone and dihydrotestosterone tissue levels in recurrent prostate cancer. Clin Cancer Res 2005;11(13):4653–4657.
6. Gonzalez FJ. Human cytochrome P450:possible roles of drug-metabolizing enzymes and polymorphic drug oxidation in addiction. NIDA Res Monogr 1991;111:202–213.
7. Waxman DJ, Attisano C, Guengerich FP, Lapenson DP. Human liver microsomal steroid metabolism: Identification of the major microsomal steroid hormone 6 beta-hydroxylase cytochrome P450 enzyme. Arch Biochem Biophys 1988;263(2): 424–436.
8. Gonzalez FJ, Lee YH. Constitutive expression of hepatic cytochrome P450 genes. FASEB J 1996;10(10):1112–1117.
9. Schmidt R, Baumann F, Knupfer H, Brauckhoff M, Horn LC, Schonfelder M, Kohler U, Preiss R. CYP3A4,CYP2C9 and CYP2B6 expression and ifosfamide turnover in breast cancer tissue microsomes. Br J Cancer 2004;90(4):911–916.
10. El-Rayes BF, Ali S, Heilbrun LK, Lababidi S, Bouwman D, Visscher D, Philip PA. Cytochrome p450 and glutathione transferase expression in human breast cancer. Clin Cancer Res 2003;9(5):1705–1709.
11. Williams JA, Phillips DH. Mammary expression of xenobiotic metabolizing enzymes and their potential role in breast cancer. Cancer Res 2000;60(17):4667–4677.
12. Finnstrom N, Bjelfman C, Soderstrom TG, Smith G, Egevad L, Norlen BJ, Wolf CR, Rane A. Detection of cytochrome P450 mRNA transcripts in prostate samples by RT-PCR. Eur J Clin Invest 2001;31(10):880–886.
13. Nishimura M, Yaguti H, Yoshitsugu H, Naito S, Satoh T. Tissue distribution of mRNA expression of human cytochrome P450 isoforms assessed by high-sensitivity real-time reverse transcription PCR. Yakugaku Zasshi 2003;123(5):369–375.
14. Fujimura T, Takahashi S, Urano T, Ogawa S, Ouchi Y, Kitamura T, Muramatsu M, Inoue S. Differential expression of estrogen receptor beta (ERbeta) and its C-terminal truncated splice variant ERbetacx as prognostic predictors in human prostatic cancer. Biochem Biophys Res Commun 2001;289(3):692–699.
15. Allred DC, Clark GM, Elledge R, Fuqua SA, Brown RW, Chamness GC, Osborne CK, McGuire WL. Association of p53 protein expression with tumor cell proliferation rate and clinical outcome in node-negative breast cancer. J Natl Cancer Inst 1993; 85(3):200–206.
16. Hesse LM, Venkatakrishnan K, Court MH, von Moltke LL, Duan SX, Shader RI, Greenblatt DJ. CYP2B6 mediates the in vitro hydroxylation of bupropion: Potential drug interactions with other antidepressants. Drug Metab Dispos 2000;28(10):1176–1183.
17. Xie W, Evans RM. Orphan nuclear receptors: The exotics of xenobiotics. J Biol Chem 2001;276(41):37739–37742.
18. Tokizane T, Shiina H, Igawa M, Enokida H, Urakami S, Kawakami T, Ogishima T, Okino ST, Li LC, Tanaka Y, Nonomura N, Okuyama A, Dahiya R. Cytochrome P450 1B1 is overexpressed and regulated by hypomethylation in prostate cancer. Clin Cancer Res 2005;11(16):5793–5801.
19. Catalona WJ, Smith DS. Cancer recurrence and survival rates after anatomic radical retropubic prostatectomy for prostate cancer: Intermediate-term results. J Urol 1998;160 (6 Pt 2):2428–2434.
20. Roehl KA, Han M, Ramos CG, Antenor JA, Catalona WJ. Cancer progression and survival rates following anatomical radical retropubic prostatectomy in 3,478 consecutive patients: Long-term results. J Urol 2004;172(3):910–914.
21. Tsunedomi R, Iizuka N, Hamamoto Y, Uchimura S, Miyamoto T, Tamesa T, Okada T, Takemoto N, Takashima M, Sakamoto K, Hamada K, Yamada-Okabe H, Oka M. Patterns of expression of cytochrome P450 genes in progression of hepatitis C virus-associated hepatocellular carcinoma. Int J Oncol 2005;27(3):661–667.
22. Kan O, Griffiths L, Baban D, Iqball S, Uden M, Spearman H, Slingsby J, Price T, Esapa M, Kingsman S, Kingsman A, Slade A, Naylor S. Direct retroviral delivery of human cytochrome P450 2B6 for gene-directed enzyme prodrug therapy of cancer. Cancer Gene Ther 2001;8(7):473–482.
23. Chen L, Waxman DJ, Chen D, Kufe DW. Sensitization of human breast cancer cells to cyclophosphamide and ifosfamide by transfer of a liver cytochrome P450 gene. Cancer Res 1996;56(6): 1331–1340.
24. Ikezoe T, Hisatake Y, Takeuchi T, Ohtsuki Y, Yang Y, Said JW, Taguchi H, Koeffler HP. HIV-1 protease inhibitor, ritonavir: A potent inhibitor of CYP3A4, enhanced the anticancer effects of docetaxel in androgen-independent prostate cancer cells in vitro and in vivo. Cancer Res 2004;64(20):7426–7431.
25. Waxman DJ, Lapenson DP, Aoyama T, Gelboin HV, Gonzalez FJ, Korzekwa K. Steroid hormone hydroxylase specificities of eleven cDNA-expressed human cytochrome P450s. Arch Biochem Biophys 1991;290(1):160–166.
26. Isaacs JT, McDermott IR, Coffey DS. The identification and characterization of a new C19O3 steroid metabolite in the rat ventral prostate: 5 Alpha-androstane-3 beta, 6 alpha, 17 beta-triol. Steroids 1979;33(6):639–657.
27. Isaacs JT, McDermott IR, Coffey DS. Characterization of two new enzymatic activities of the rat ventral prostate: 5 Alpha-androstane-3 beta, 17 beta-diol 6 alpha-hydroxylase and 5 alpha-androstane-3 beta, 17 beta-diol 7 alpha-hydroxylase. Steroids 1979;33(6):675–692.
28. Sundin M, Warner M, Haaparanta T, Gustafsson JA. Isolation and catalytic activity of cytochrome P-450 from ventral prostate of control rats. J Biol Chem 1987;262(25):12293–12297.
29. Goodwin B, Moore LB, Stoltz CM, McKee DD, Kliewer SA. Regulation of the human CYP2B6 gene by the nuclear pregnane X receptor. Mol Pharmacol 2001;60(3):427–431.
30. Pascussi JM, Gerbal-Chaloin S, Fabre JM, Maurel P, Vilarem MJ. Dexamethasone enhances constitutive androstane receptor expression in human hepatocytes: Consequences on cyto-chrome P450 gene regulation. Mol Pharmacol 2000;58(6):1441–1450.

Characterization and Identification of a Steroid Receptor-Binding Protein, SRB-RGS

Mitsunori IKEDA,*[a] Satoshi INOUE,[b,c] Masami MURAMATSU,[c] and Yohsuke MINATOGAWA[a]

[a] Department of Biochemistry, Kawasaki Medical School; 577 Matsushima, Kurashiki, Okayama 701–0192, Japan: [b] Department of Geriatrics, Graduate School of Medicine and Faculty of Medicine, University of Tokyo; 7–3–1 Hongo, Bunkyo-ku, Tokyo 113–0033, Japan: and [c] Research Center for Genomic Medicine, Saitama Medical School; 1397–1 Inariyama, Yamane, Hidaka 350–1241, Japan.

Received June 30, 2006; accepted April 8, 2007; published online April 10, 2007

We cloned the cDNA of a novel steroid receptor-binding protein, SRB-RGS, which suppressed the estrogen receptor (ER)α-mediated and other promoter-driven transcriptional activities. This study revealed the interaction between the full-length SRB-RGS and full-length ERα or ERβ by a coimmunoprecipitation assay. The full-length SRB-RGS and full-length ERα interacted in COS-7 cell by a mammalian two-hybrid system. The interaction between intrinsic SRB-RGS and ERs in the nuclear ER extract from the rat uteri was observed by the gel-shift assay. These results strongly suggested that SRB-RGS interacts with ERs bound to DNA (estrogen response element) in the nuclei of the cells. SRB-RGS suppressed very efficiently the ERα-, ERβ-, and ERα+ERβ-mediated transcriptional activities. Green fluorescence of enhanced green fluorescence protein (EGFP)-tagged SRB-RGS was localized both in the nucleus and in the cytoplasm. Intrinsic SRB-RGS was immunostained in the nucleus and the cytoplasm of HeLa cells. The putative SRB-RGS deduced from cDNA sequence was identified by the immunostaining and Western blotting by using the anti-SRB-RGS antibody. Overexpression of SRB-RGS induced the cell death in the HeLa cells. The nucleotide sequence of SRB-RGS cDNA that we cloned previously is identical with that of the newly isolated RGS3 cDNA. SRB-RGS could interact with ERs bound DNA in the nuclei of the cells and suppressed the ERs-mediated transcriptional activities.

Key words estrogen receptor; gene expression; transcriptional suppression; localization; cell death; RGS3

The nuclear hormone receptors are a superfamily of ligand-inducible transcription factors. They include the receptor proteins for steroids, thyroid hormone, vitamin D, and retinoids. Steroid hormone receptors are structurally related and composed of six major functional domains. Domain A/B in the NH_2-terminal region of the protein is the constitutive activation 1 (AF-1). Domain C, the DNA-binding domain, is arranged in two zinc-stabilized DNA-binding finger motifs. Region D contains a nuclear localization signal. The ligand-binding and ligand-dependent transcriptional activation function 2 (AF-2) is located in domain E/F of the COOH-terminal region of the protein.[1—3] For the activation of transcription, steroid hormone receptors recruit coactivators such as SRC-1/p160, p300/CBP, ARA70, Tip60, and RIP140, through binding to AF-1 and AF-2 of the receptors. This kind of coactivator recruits histone acetyltransferase (HAT) or bear HAT activity on itself. Recruitment of HAT allows the local decondensation of chromatin. In the next step, the DRIP/TRAP complex binds to the AF-2 of the receptor and mediates transcriptional activation. This kind of coactivator does not recruit HAT. Thus, these coactivators facilitate the transcription process.[4—9] The thyroid hormone receptor (TR) and retinoid X receptor (RXR) in the absence of ligand bind to the corepressors, such as N-CoR and SMRT, respectively, suppressing transcriptional activity. The corepressors recruit histone deacetylase (HDAC).[10—13] The chromatin-modifying complexes, ATP-dependent remodeling complexes and HAT or HDAC complexes regulate chromatin structure and transcription so that they might be coordinated to create a DNA template that is accessible to the general transcription apparatus.[14]

We employed a yeast two-hybrid system for cloning the cDNA of the protein that interacted with domains C and D of the rat estrogen receptorα (rERαC/D) from the rat ovary cDNA library and cloned the cDNA of a novel steroid receptor-binding (SRB) protein bearing the regulator of the G-protein signaling (RGS) domain[15] at the COOH-terminal, designated as SRB-RGS. RGS proteins are GTPase accelerating proteins, which interact with the Gα-subunits that are linked to seven transmembrane G-protein coupled receptor. SRB-RGS bears a PDZ domain that is a multi-functional protein–protein interaction module that plays important roles in organizing signal transduction complexes, clustering membrane proteins, and maintaining cell polarity at the NH_2-terminal, as well.[16,17] rERαC/D interacted *in vitro* with partial SRB-RGS1-495 amino acid (a.a.). SRB-RGS suppressed the transcriptional activities of ERα and the other promoters.[18]

We could show that the full-length SRB-RGS interacted with either the full-length ERα or ERβ by a coimmunoprecipitation assay. The full-length SRB-RGS and full length ERα interacted in COS-7 cell by a mammalian two-hybrid system. The interaction between intrinsic SRB-RGS and ERs in the nuclear ER extract from the rat uteri was suggested by the gel-shift assay. The human (h) ERα-, hERβ-, hERα+hERβ-mediated transcriptional activities were suppressed by overexpression of SRB-RGS. Enhanced fluorescence protein (EGFP)-tagged SRB-RGS was localized in the nucleus and the cytoplasm of the HeLa cells and the COS-7 cells. Similar results were shown by immunostaining of the HeLa cells. Intrinsic SRB-RGS was identified by the immunostaining and Western blotting. Overexpression of SRB-RGS induced the cell death in the HeLa cells. SRB-RGS could interact with ERs bound DNA in the nucleus and suppressed the ERs-mediated transcriptional activities.

* To whom correspondence should be addressed. e-mail: ikeda@bcc.kawasaki-m.ac.jp

MATERIALS AND METHODS

Materials Anti-hERα rabbit polyclonal antibody HC-20, raised against a peptide mapping at the COOH-terminus of ERα of human origin and anti-hERβ antibody N-19, goat polyclonal antibody raised against a peptide mapping at the NH_2-terminus of ERβ of human origin, were purchased from Santa Cruz Biotechnology (Santa Cruz, CA, U.S.A.). [^{35}S]methionine was purchased from Amersham Biosciences Co. (Piscataway, NJ, U.S.A.). [α-^{33}P]dATP was purchased from Perkin Elmer Life and Analytical Sciences (Boston, MA, U.S.A.).

Preparation and Purification of the Antiserum against the SRB-RGS Peptide The anti-SRB-RGS peptide antiserum was prepared by Sawady Technology Co. (Tokyo, Japan) immunizing a rabbit. The immune serum was assayed by enzyme-linked immunoassay with detection at greater than 10000-fold dilution by the manufacturer. The immune and the preimmune sera were purified on protein A Sepharose™ CL-4B (Amersham Biosciences Co.). The purified sera are called as the anti-SRB-RGS antibody and the preimmune serum, respectively.

Construction of Plasmids The expression vectors of SRB-RGS, pcDNASRB-RGS or β-galactosidase (β-gal), pcDNAβ-gal (pCMVβ-gal) were constructed by inserting SRB-RGS cDNA, β-gal cDNA from pCH110, respectively into the malti-cloning site (MCS) of pcDNA3 (Invitrogen Co., Groningen, The Netherlands) driven by a cytomegalovirus (CMV) promoter in mammalian cells and by the T7 promoter in the *in vitro* transcription translation system.[18] The expression vector for EGFP-tagged SRB-RGS, pEGFP-SRB-RGS was constructed by inserting the PCR-amplified cDNA fragment of SRB-RGS into the HindIII site in the MCS of pEGFP-C1 (Clontech Co., Palo Alto, CA, U.S.A.). The expression vectors of DsRed1-tagged hERα and hERβ, pDsRed-hERα and pDsRed-hERβ were constructed by inserting PCR-amplified cDNA fragments from pCXN2-hERα and pCXN2-hERβ,[19] respectively into the MCS of pDsRed1-C1 (Clontech Co.). The construction of the expression vectors of hERα, pcDNA-hERα, and hERβ, pcDNA-hERβ were constructed by inserting PCR-amplified cDNA fragments from pCXN2-hERα and pCXN2-hERβ, respectively into the MCS of pcDNA3. The constructions of pASrERαC/D, pASrERα and pACTrERαC/D were described previously.[18,20] pACTSRB-RGS was constructed by inserting the EcoRI cDNA fragment of pcDNASRB-RGS into the EcoRI site in the MCS of pACT2 after adding 8 nucleotides at the NcoI site. pACTSRB-RGS 1-495 a.a. was constructed by inserting a PCR-amplified cDNA fragment of SRB-RGS 1-495 a.a. into the EcoRI site in the MCS of pACT2. pASSRB-RGS was constructed by inserting the EcoRI fragment of pcDNASRB-RGS into the EcoRI site in the MCS of pAS2-1. The expression vectors of the fusion proteins of GAL4 DNA-binding domain (GAL4 DNA-BD) and hERα, pM-hERα and VP16 activation-domain (VP16AD) and SRB-RGS, pVP16SRB-RGS were constructed by inserting PCR-amplified cDNA fragments from pcDNA-hERα and pcDNASRB-RGS, respectively into the MCS of the expression vectors of GAL4 DNA-BD, pM and VP16AD, pVP16 (Clontech Co.), respectively.

An Interaction Study between SRB-RGS and ERs by a Yeast Two-Hybrid System A yeast two-hybrid interaction study was performed as mentioned previously.[18,20,21] Briefly, the colonies of *Saccharomyces cerevisiae* Y187 (Y187) transfected with pAS2-1, pASrERα, pASSRB-RGS and pLAM5′-1 and the colonies of *Saccharomyces cerevisiae* CG-1945 (CG-1945) transfected with pACT2, pACTrERα, and pACTSRB-RGS 1-495 a.a. were incubated together in the same YPD medium (20 g/l polypeptone, 10 g/l yeast extract, 20 g/l glucose) at 30 °C for 10 h with shaking, and an aliquot of the mating culture was placed on a synthetic dropout minimal medium (SD)/-leucine/-tryptophane/-histidine+5 mM 3-amino-1,2,4-triazole (3-AT) plate in the absence or presence of 10^{-6} M estradiol. The transformants were assayed for β-gal activity by the colony-lift filter assay. Interacting positives turned blue.

***In Vitro* Interaction between SRB-RGS and ERs by Coimmunoprecipitation** [^{35}S]methionine-labeled proteins were prepared by using an *in vitro* transcription translation system. pcDNASRB-RGS+pcDNA-hERα or pcDNASRB-RGS+pcDNA-hERβ as the templates and [^{35}S]methionine were added to the reaction mixture (TnT^{R} Quick Coupled Transcription/Translation System, Promega Co., Madison, WI, U.S.A.) in the respective tubes. The each reaction mixture was incubated at 30 °C for 1.5 h and then with protein G PLUS-agarose (Santa Cruz Biotechnology) for 1 h on ice. After centrifugation, the supernatants were incubated with the anti-hERα antibody HC-20, the anti-hERβ antibody N-19 or anti-SRB-RGS antibody for 2 h on ice and then with protein G PLUS-agarose for 1 h on ice. The protein G PLUS-agarose was washed with 10 mM Tris–HCl, 1 mM EDTA (pH 7.4) (TE) containing 0.4 M NaCl and 0.1% Nonidet P-40 (for SRB-RGS+hERβ) or 10 mM Tris–HCl, 1 mM EDTA (pH 7.4) (TE) containing 0.2 M NaCl and 0.05% Nonidet P-40 (for SRB-RGS+hERα). The labeled proteins bound to the protein G PLUS-agarose were analyzed by 9% SDS-polyacrylamide gel electrophoresis (PAGE) and an autoradiography by using the Fluoro image analyzer FLA-3000 (Fuji Film Co., Tokyo, Japan).

Cell Culture and Transfection COS-7 cells and HeLa cells were purchased from The Institute of Physical and Chemical Research (RIKEN) (Wako, Japan). They were routinely maintained in Dulbecco's modified Eagle's minimal essential medium (DMEM) (Sigma Co., St. Louis, MO, U.S.A.) supplemented with 10% fetal bovine serum (FBS) (Medical & Biological Laboratories Co., Nagoya, Japan). The cells were maintained in 5% CO_2 at 37 °C. The COS-7 cells or the HeLa cells in screw-capped flasks (25 cm^2) or 35-mm dishes (10.8 cm^2) were transiently transfected with plasmids by lipofectamine2000 (Invitrogen Co.). The cells were incubated for 48 h after transfection.

Chloramphenicol Acetyltransferase Assay The chloramphenicol acetyltransferase (CAT) assay for ER transcriptional activity, using a FAST CAT Yellow (deoxy) CAT assay kit (Molecular Probes, Eugene, OR, U.S.A.), and the β-gal assay were performed as mentioned previously.[18] Briefly, the medium for COS-7 cells in a screw-capped flask (25 cm^2) was replaced by phenol red-free MEM (Nissui Pharmaceutical Co., Tokyo, Japan) supplemented with 10% dextran-coated charcoal-treated (DCC) FBS for 48 h before transfection. The COS-7 cells were cotransfected with plasmids as indicated and incubated for 48 h in the presence of 10^{-7} M

estradiol after transfection. The cell extract was prepared according to the manufacturer's manual. A portion of the cell extract was incubated with fluorescent deoxychloramfenicol substrate and acetyl CoA (Sigma Co.) at 37 °C for 2 h. The acetylated derivative and the substrate were quantified by measuring the absorbance using the fluorescence spectrophotometer Model F-3010 (Hitachi Co., Tokyo, Japan). For the β-gal assay, the other portion of the cell extract was incubated with *o*-nitrophenyl β-galactopyranoside at 37 °C for 30 min. The relative CAT activities were calculated according to the manufacturer's manual and normalized by β-gal activities. The CAT activity for the cells cotransfected with the empty plasmid, pcDNA3 instead of pcDNA-hERα (or pcDNA-hERβ) was subtracted from each CAT activity.

Quantitative Real-Time RT-PCR pcDNA-hERα (or pcDNA-hERβ), pEREtkCAT and pcDNAβ-gal were cotransfected with pcDNASRB-RGS (or pcDNA3) to COS-7 cells and incubated under the same condition as mentioned below in Fig. 2 (the CAT assay for the ER transcriptional activites). Total RNA was prepared by RNeasy Plus Mini kit (Qiagen GmbH, Hilden, Germany) according to the manufacturer's manual from 2.5×10^6 COS-7 cells. Briefly, the homogenized lysate was centrifuged in a DNA Eliminator spin column to eliminate contaminating DNA and then in a RNeasy spin column to get total RNA. A_{260}/A_{280} value was approximately 2.2. The total RNA was converted to cDNA by iScript cDNA synthesis kit (Bio-Rad Co., Hercules, CA, U.S.A.) using a modified MMLV-derived reverse transcriptase, oligo (dT) and random hexamer primers. SYBR green-based real-time RT-PCR was carried out by SYBR GREEN PCR Master Mix (Applied Biosystems, Warrington, U.K.) using Mx3000P™ Multiplex Quantitative PCR System (Stratagene Co., La Jolla, LA, U.S.A.). The following primer pairs were used: 5′-ATC AGG ATA TGT GGC GGA TGA-3′ (forward) and 5′-CTG ATT TGT GTA GTC GGT TTA TGC A-3′ (reverse) for amplification of β-gal, 5′-CCA CCA ACC AGT GCA CCA TT-3′ (forward) and 5′-GGT CTT TTC GTA TCC CAC CTT TC-3′ (reverse) for amplification of hERα and: 5′-AGA GTC CCT GGT GTG AAG CAA G-3′ (forward) and 5′-GAC AGC GCA GAA GTG AGC ATC-3′ (reverse) for amplification of hERβ. The plasmids pcDNAβ-gal, pcDNA-hERα and pcDNA-hERβ were used as standards of quantification for β-gal, hERα and hERβ cDNAs, respectively. Reactions were incubated at 95 °C for 10 min followed by 40 cycles of 95 °C for 15 s and 60 °C for 1 min. Controls incubated no-reverse transcriptase reactions in which reverse transcriptase were omitted from the reverse transcriptase reaction.

Mammalian Two-Hybrid System Mammalian two-hybrid assay for interaction between ERα and SRB-RGS was performed using Mammalian Matchmaker Two-Hybrid Assay kit (Clontech Co.). Briefly, COS-7 cells were cotransfected with plasmids as indicated and incubated in the absence or presence of 10^{-7} M estradiol. The cell extracts were incubated with fluorescent deoxychloramfenicol substrate and acetyl CoA as mentioned above. The relative CAT activities were normalized by β-gal activities as mentioned above.

Observation of Subcellular Localization of SRB-RGS and TUNEL-Positive Cells by Confocal Laser-Scanning Microscopy The HeLa cells or COS-7 cells in 35-mm dishes (10.8 cm^2) were grown on glass cover slips in phenol red-free MEM supplemented with 10% DCC FBS, and the plasmids were transiently cotransfected by lipofectamine2000. They were incubated for 48 h in the presence or absence of 10^{-7} M estradiol or 10 μM Z-VAD-FMK (the caspases inhibitor) (Peptide Institute Inc., Minoh, Osaka, Japan) after transfection. The cells washed with PBS and fixed in 4% paraformaldehyde for 1 h. After the cover slips were mounted on to glass sides after or without propidium iodide (PI) staining of the cells, the cells were viewed on a confocal laser-scanning microscopy Model Fluoview FV300 (Olympus Co., Tokyo, Japan).

The ApoTag^R Red *In Situ* Apoptosis Detection kit (Intergen Co., Purchase, NY, U.S.A.) was used for the assessment of DNA fragmentation in the cells transfected with the plasmids after fixation of the cells on glass cover slips. Briefly, DNA fragments, which had been labeled with the digoxigenin-nucleotide, were then allowed to bind an anti-digoxigenin antibody conjugated to Rhodamine. The cells were viewed on a confocal laser-scanning microscopy as mentioned above.

Immunostaining of the Cells HeLa cells were grown on glass cover slips in 35-mm dishes and fixed in 4% paraformaldehyde for 1 h. After permiabilization with 2% Triton X-100 in PBS for 10 min. at room temperature, the cells were blocked with 20% FBS in PBS and incubated with the anti-SRB-RGS antibody (or the preimmune serum) and then the fluorescein-5-isothiocyanate (FITC)-conjugated goat IgG to rabbit immunoglobulin (IgG, IgA, IgM) (ICN pharmaceuticals, Aurora, OH, U.S.A.) followed by PI staining. They were observed on a confocal laser-scanning microscopy as mentioned above.

SDS-PAGE Analysis of [^{35}S]Methionine-Labeled SRB-RGS Expressed in COS-7 Cells Transfected with pcDNASRB-RGS COS-7 cells at 48 h after transfection with pcDNASRB-RGS or the empty plasmid, pcDNA3 were labeled for 4 h in methionine- and cystine-free DMEM (Gibco/Invitrogen Co., Carlsbad, CA, U.S.A.) containing [^{35}S]methionine (100 μCi/ml). The labeled cells were lysed in a solubilization buffer containing 10 mM Tris–HCl (pH 7.4), 0.15 M NaCl, 1% Nonidet P-40, 0.1% SDS, a protease inhibitor cocktail for mammalian tissues (Sigma Co.), designated as the whole cell lysate. The anti-SRB-RGS antibody was added to the whole cell lysate, and incubated for 1 h on ice. The immune complexes were adsorbed to protein G PLUS-agarose, washed extensively with a washing buffer [10 mM Tris–HCl (pH 7.4), 0.15 M NaCl, 0.1% Nonidet P-40, 0.1% SDS, and the protease inhibitor cocktail], and then analyzed with 7% SDS-PAGE followed by an autoradiography as mentioned above.

Western Blotting Analysis HeLa cells without transfection of any plasmids were lysed in the solubilization buffer as mentioned above and dialyzed against TE. The lysate was subjected on 7% SDS-PAGE and transferred to a nitrocellulose membrane (Bio-Rad Co.). The analysis was performed with ECL plus Western blotting detection system (Amersham Biosciences UK Limited, Little Chalfont, U.K.). Briefly, the membrane was immersed in 5% non-fat dried milk, 0.1% Tween 20 in PBS and incubated with the anti-SRB-RGS antibody and then peroxidase-linked anti-rabbit IgG. Peroxydase activity was developed according to the manufacturer's manual. The chemiluminescent signal of the band was visualized

Table 1. An Interaction Study between the Estrogen Receptor and SRB-RGS by a Yeast Two-Hybrid System

Plasmid 1 in Y-187	Plasmid 2 in CG-1945							
	pACT2		pACTrERα		pACTSRB-RGS		pACTSRB-RGS 1-495 a.a.	
	$-E_2$	$+E_2$	$-E_2$	$+E_2$	$-E_2$	$+E_2$	$-E_2$	$+E_2$
pAS2-1	−	−	−	−	nd		nd	
pASrERα	nd		−	+	nd		+	+
pASSRB-RGS	nd		−	−	nd		nd	
pASrERαC/D	nd		−	−	±	±	+	+
pLAM5′-1	nd		nd		nd		−	−

Saccharomyces cerevisiae Y187 and CG-1945 were transfected with plasmids 1 and 2, respectively, followed by yeast mating. The growth and β-galactosidase (β-gal) assay of the cells were determined as described previously.[18] The growth was performed in the presence ($+E_2$) or absence ($-E_2$) of 10^{-6} M estradiol. The growth and β-gal assay of yeast cells were expressed as positive (+), negative (−), and faintly positive (±). rERαC/D: the bait for a yeast two-hybrid screening. SRB-RGS 1-495 a.a.: the open reading flame of the cDNA fragment (clone4-32) isolated by a yeast two-hybrid screening. pLAM5′-1: human lamin $C_{(66\text{-}230)}$ in pAS2-1 as a control bait. nd: not determined.

using a Lumino image analyzer LAS-1000 plus (Fuji Film Co.).

Gel-Shift Assay The gel-shift assay was performed as mentioned previously.[2,20]

Animal and Tissue Preparation: Female SD rats (8 week-old) were obtained from Charles River Co. (Yokohama, Japan), and were sacrificed by cervical dislocation. The uteri were removed and immediately frozen in liquid nitrogen. They were used immediately or stored at −80 °C before use. These experiments were approved by Animal Research Committee of Kawasaki Medical School and conducted according to the "Guide for the Care and Use of Laboratory Animals" of Kawasaki Medical School.

Preparation of the Nuclear Receptor Fraction from the Rat Uteri: The operations were carried out at 0—4 °C. The nuclear receptor fraction was prepared following treatment of the rats with estradiol (100 μg/kg). The uteri were homogenized with TEGMPi buffer[2] and filtered through Nytex (100—124 μm). The filtrate was centrifuged at 2500×***g*** for 10 min. The pellet was washed twice with homogenization buffer and resuspended in the buffer containing 0.4 M KCl and allowed to extract for 30 min. The suspension was centrifuged at 105000×***g*** for 50 min.

Synthetic Oligonucleotides: A wild type 25-base pair synthetic oligonucleotide containing a *Xenopus* vitellogenin A2 estrogen response element (VRE) were prepared as followed: The synthetic oligonucleotide 5′-TCAGGTCACTGTGACCTGACTTTGG-3′ was annealed to the complementary primer 5′-CCAAAGTC-3′. [^{33}P]VRE or the unlabeled VRE was synthesized by end-filling of the annealed oligonucleotide with Klenow fragment (Takara Co., Kusatsu, Japan) in the presence of 20 μM each of dCTP, dGTP, dTTP, dATP with or without 5 μM of [α-^{33}P]dATP, respectively.

Gel-Shift Assay: The nuclear receptor fraction were incubated with [^{33}P]VRE, electrophoresed through non-denaturing PAGE (5.6%), and autoradiographed as mentioned above.

RESULTS

Interaction Study of the Estrogen Receptors and SRB-RGS Yeast Two-Hybrid Assay: We examined the interaction between ERs and SRB-RGS by a yeast two-hybrid system. Full-length rERα (or rERαC/D, the bait for a yeast two-hybrid screening) and SRB-RGS 1-495 a.a. [the open reading frame of the cDNA fragment (clone4-32) isolated by a yeast two-hybrid screening] interacted in both the absence and presence of estradiol in the culture medium of the yeast two-hybrid system. No interaction between full-length rERα and full-length SRB-RGS was observed in this system (Table 1).

Coimmunoprecipitation Assay: We examined whether [^{35}S]methionine-labeled SRB-RGS, hERα or hERβ were translated correctly by an *in vitro* transcription and translation system adding pcDNASRB-RGS, pcDNA-hERα or pcDNA-hERβ, respectively, as the templates and [^{35}S]methionine to the reaction mixture containing the rabbit reticulocyte lysate. The labeled products immunoprecipitated by the respective antibodies and protein G-agarose showed their apparent molecular weights on SDS-PAGE (data not shown), suggesting that they were translated correctly in this system.

The interaction study of full-length SRB-RGS and full-length ERs was examined by a coimmunoprecipitation assay. Estradiol was not added to the medium for the interaction study using immunoprecipitation assay on the basis of the above observation by a yeast two-hybrid system. [^{35}S]methionine-labeled SRB-RGS and hERα were synthesized in the same reaction mixture of an *in vitro* transcription and translation system and immunoprecipitated by an anti-hERα antibody HC-20 or an anti-SRB-RGS antibody, and analyzed by SDS-PAGE and autoradiography. Similarly, an interaction between hERβ and SRB-RGS was examined. [^{35}S]methionine-labeled SRB-RGS and hERβ synthesized as mentioned above were immunoprecipitated by the anti-hERβ antibody N19 or the anti-SRB-RGS antibody, and analyzed by SDS-PAGE and autoradiography. SRB-RGS or ERs were coimmunoprecipitated by the anti-SRB-RGS antibody (Fig. 1A lanes 2, 6), anti-hERα antibody (Fig. 1A lane 3) or anti-hERβ antibody (Fig. 1A lane 7), respectively, whereas they were hardly coimmunoprecipitated by the vehicle that contained the preimmune serum (Fig. 1A lanes 1, 5). These observations showed that full-length SRB-RGS bound to either full-length hERα or hERβ *in vitro*.

Mammalian Two-Hybrid Assay: The interaction of full-length SRB-RGS and full-length hERα in the COS-7 cells was examined by a mammalian two-hybrid assay in the absence or presence of estradiol. As indicated at the bottom of Fig. 1B, the expression vectors of the fusion proteins of GAL4 DNA-binding domain (GAL4 DNA-DB) and hERα, pM-hERα (or an empty vector, pM) and VP16 activation-domain (VP16 AD) and SRB-RGS, pVP16 SRB-RGS (or an empty vector, pVP16) were also cotransfected with the re-

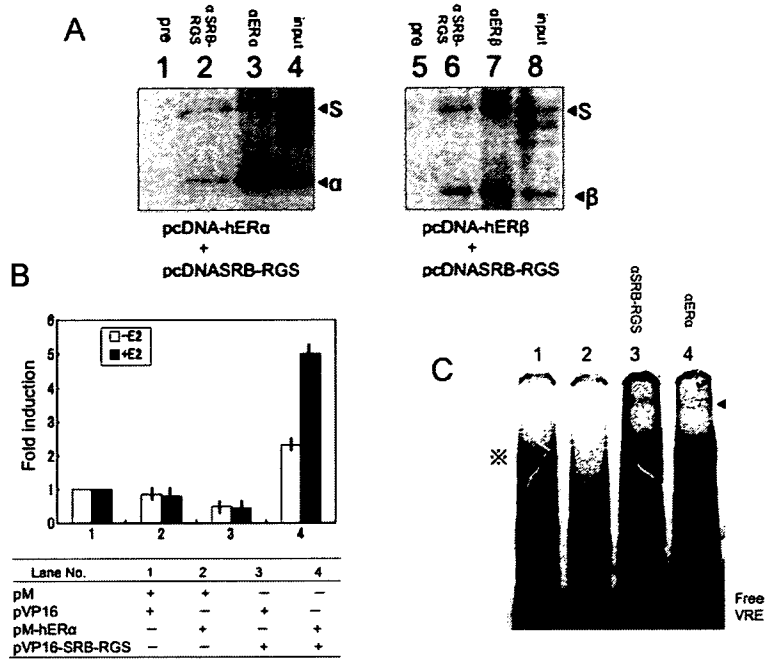

Fig. 1. An Interaction Study between SRB-RGS and the Estrogen Receptors

(A) Coimmunoprecipitation assay: [^{35}S]methionine-labeled proteins were prepared by using either pcDNASRB-RGS+pcDNA-hERα (lanes 1—4) or pcDNASRB-RGS+pcDNA-hERβ (lanes 5—8) as templates in respective tubes with the *in vitro* transcription and translation system. Respective reaction mixtures were incubated with the preimmune serum (pre; lanes 1, 5), the anti-SRB-RGS antibody (αSRB-RGS; lanes 2, 6), the anti-hERα antibody HC-20 (αERα; lane 3), or the anti-hERβ antibody N19 (αERβ; lane 7), precipitated with the protein G PLUS-agarose, and washed with TE containing 0.2 M NaCl and 0.05% Nonidet P-40 (lanes 1—3) or TE containing 0.4 M NaCl and 0.1% Nonidet P-40 (lanes 5—7). The bound proteins were analyzed by SDS-PAGE and autoradiography. Lanes 4 and 8 represent one ninth of the total amount of input [^{35}S]methionine-labeled proteins in each reaction tube. S: SRB-RGS. α: hERα. β: hERβ. (B) A mammalian two-hybrid assay: An interaction study between hERα and SRB-RGS was performed by mammalian two-hybrid system. Briefly, COS-7 cells were cotransfected with plasmids as indicated and incubated in the absence (white bar) or presence (black bar) of 10^{-7} M estradiol (E_2). The cell extracts were incubated with fluorescent deoxychloramfenicol substrate and acetyl CoA. The relative CAT activities were normalized by β-gal activities. (C) Gel shift assay: The effect of the anti-SRB-RGS antibody on VRE-binding nuclear ERs was examined by the gel-shift assay as described under "Materials and Methods". ERs-[^{33}P]VRE complexes were formed prior to addition of preimmune serum (lanes 1, 2), the anti-SRB-RGS antibody (αSRB-RGS; lane 3), and the anti-hERα HC-20 (αERα; lane 4). Lane 2 also contains large excess of unlabeled VRE. The asterisk indicates specific ERs-VRE bands. The arrowhead indicates antibody-shifted ERs-VRE complexes.

porter plasmid, pG5CAT which contains the CAT gene downstream of five consensus GAL4 binding sites and the minimal adenovirus E1b promoter to COS-7 cells. The interaction between hERα and SRB-RGS was expressed as relative CAT activity normalized by β-gal activity. The CAT activity remained low when cells were transfected with the empty plasmids (pM and pVP16AD), or when either of these plasmids was transfected together with pM-hERα or pVP16 SRB-RGS. In contrast, when pM-hERα was transfected together with pVP16 SRB-RGS, the CAT activities of the reporter were induced approximately 5-fold and 2.3-fold in the presence or absence of 10^{-7} M estradiol, respectively (Fig. 1B). In the presence and absence of 10^{-7} M estradiol, SRB-RGS interacted with hERα in the nucleus of the COS-7 cell.

Gel-Shift Assay: The interaction of intrinsic SRB-RGS and ERs in the nuclear receptor fraction from the rat uteri was examined by the gel-shift assay. The nuclear receptor fraction incubated with [^{33}P]VRE was separated from the free oligonucleotide on nondenaturing PAGE. Retarded bands were observed (the asterisk in Fig. 1C lane 1). The band disappeared as a result of competition with excess of unlabeled VRE (lane 2). A super-shift of the retarded bands was observed by incubation with the anti-SRB-RGS antibody or anti-ERα antibody HC-20 (the arrow-head lanes 3 or 4, respectively). The [^{33}P]VRE-binding band included SRB-RGS and ERα, suggesting that SRB-RGS interacted with ERα bound to VRE.

Effects of SRB-RGS on the ERα-, ERβ- and ERα+ERβ-Mediated Transcriptional Activities The COS-7 cells were transfected with pcDNASRB-RGS (or the empty plasmid, pcDNA3) and labeled with [^{35}S]methionine. The whole cell lysates of the COS-7 cells were immunoprecipitated with the anti-SRB-RGS antibody and the protein G PLUS-agarose. The precipitates were analyzed with SDS-PAGE and autoradiography. The band of the [^{35}S]methionine-labeled protein in the immunoprecipitate had the same mobility as [^{35}S]methionine-labeled SRB-RGS prepared by an *in vitro* transcription translation system. There was no band corresponding to the mobility of SRB-RGS in the lysate of the cells transfected with pcDNA3. In the COS-7 cells transfected with pcDNASRB-RGS, the SRB-RGS protein was translated with the correct amino acid sequence (data not shown).

Both ERα and ERβ are coexpressed in the same cells of estrogen target tissues. In some target tissues, each ER is distributed separately in the different cells.[22,23] We examined the effects of SRB-RGS overexpression on the ERα-, ERβ-, and ERα+ERβ-mediated transcriptional activities in COS-7 cells. We introduced the smallest and still effective amount of pcDNASRB-RGS to suppress the ERs-mediated transcriptional activities. In this condition, the CMV promoter-driven transcriptional activity (the CMV promoter-driven expression of β-gal) was not suppressed (data not shown). Therefore, the expression vector of β-gal driven by CMV promoter, pcDNAβ-gal was cotransfected to normalize transfection efficiency. As indicated at the bottom of Fig. 2, the expression

vectors of hERα, pcDNA-hERα and/or hERβ, pcDNA-hERβ (or the empty plasmid of them, pcDNA3) and the reporter plasmid for ERs-mediated transcriptional activities, pEREtkCAT were also cotransfected with the expression vector of SRB-RGS, pcDNASRB-RGS (or the empty plasmid, pcDNA3) to COS-7 cells. Using the reporter plasmids pEREtkCAT, it was demonstrated that, among hERα, hERβ, and hERα+hERβ, hERα had the strongest transcriptional activity. (Fig. 2 No. 1), hERβ had the weakest one (Fig. 2 No. 3), and hERα+hERβ had the middle-range one (Fig. 2 No. 5). ERβ inhibits ERα-mediated transcription in the presence of ERα, whereas, in the absence of ERα, it can partially replace ERα.[24] Our results (Fig. 2 Nos. 1, 3, 5) are consistent with theirs. The hERα-, hERβ-, hERα+hERβ-mediated transcriptional activities were suppressed to 41, 21, and 25%, respectively by overexpression of SRB-RGS (Fig. 2 Nos. 2, 4, and 6, respectively). SRB-RGS suppressed very effectively on the transcriptional activities of ERs, especially ERβ.

pcDNA-hERα (or pcDNA-hERβ) and pEREtkCAT were cotransfected with pcDNASRB-RGS (or pcDNA3) and pcDNAβ-gal to normalize transfection efficiency to COS-7 cells as indicated above. Quantitative real-time RT-PCR was performed to examine the effects of introduction of pcDNASRB-RGS on the expression of hERα and hERβ mRNAs. When the mRNA quantity in the cells transfected with pcDNA3 is represented as 100% in each ER, the means±S.D. of three independent experiments in the values in the cells transfected with pcDNASRB-RGS are 120±50% for hERα and 104±27% for hERβ. Introduction of pcDNASRB-RGS to the cells did not affect significantly the expression of hERα and hERβ mRNAs, suggesting that the suppression effects of SRB-RGS on the ERs-mediated transcriptional activities were not due to decrease of ERs expression in the COS-7 cells.

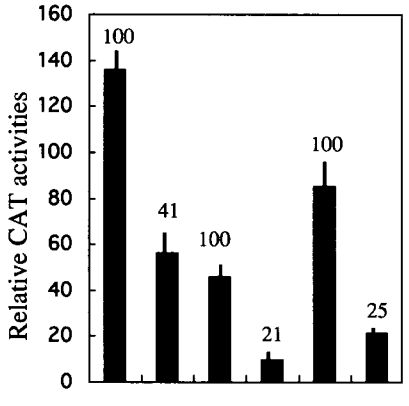

No.	1	2	3	4	5	6
pcDNA-hERα	0.01	0.01	-	-	0.005	0.005
pcDNA-hERβ	-	-	0.01	0.01	0.005	0.005
pEREtkCAT	1	1	1	1	1	1
pcDNA3	0.2	-	0.2	-	0.2	-
pcDNA SRB-RGS	-	0.2	-	0.2	-	0.2
pCMVβ-gal	0.01	0.01	0.01	0.01	0.01	0.01

Fig. 2. Effects of SRB-RGS Overexpression on ERα-, ERβ-, and ERα+ERβ-Mediated Transcriptional Activities

The COS-7 cells were transiently transfected with plasmids as indicated at the bottom. The empty plasmid, pcDNA3 was added to obtain the same input DNA amount. pcDNAβ-gal was cotransfected to normalize transfection efficiency. After transfection, the cells were incubated for 48 h in the presence of 10^{-7} M estradiol. The CAT activity for the cells cotransfected with the empty plasmid, pcDNA3 instead of pcDNA-hERα and/or pcDNA-hERβ was subtracted from each CAT activity. The numbers on top of the bars in the graphs represent the percent activity for each ER group. In each ER group, the activity in the cells transfected with pcDNA3 is represented as 100%. Values are the means±S.D. of three independent experiments.

Subcellular Localization and Identification of SRB-RGS To elucidate the subcellular localization of SRB-RGS, the expression vector of EGFP-tagged SRB-RGS, pEGFPSRB-RGS, was cotransfected with (B) or without (A) the expression vectors of DsRed1-tagged hERα or hERβ, pDsRed-hERα or pDsRed-hERβ, respectively, to HeLa cells (A) or COS-7 cells (B), as indicated in Fig. 3. Transfection of pcDNASRB-RGS (3 μg) or pEGFPSRB-RGS (3 μg) to HeLa cells induced the cell death as mentioned below in Fig. 4. Therefore, relatively small amount of the plasmid (0.2 μg) was transfected to the HeLa cells. Fluorescence was observed by a confocal laser-scanning microscopy after PI staining (Fig. 3A). Green fluorescence of EGFP-tagged SRB-RGS was observed both in the nucleus stained by PI and in the cytoplasm, but not in the plasma membrane, of the HeLa cells. By even small amount of pEGFPSRB-RGS, some HeLa cells showed the appearance of cell shrinkage (an apoptotic appearance). Therefore, pEGFPSRB-RGS (2 μg) was cotransfected to COS-7 cells with pDsRed-hERα (2 μg) or pDsRed-hERβ (2 μg). Green fluorescence of EGFP-tagged SRB-RGS was observed both in the nucleus, where hERα or hERβ localized, and in the cytoplasm, of the COS-7 cells (Fig. 3B). Subcellular localization of SRB-RGS was similar despite the presence or absence of ERs and/or estradiol in the HeLa cells and COS-7 cells.

We examined subcellular localization of intrinsic SRB-RGS and identification of intrinsic SRB-RGS by immunostaining of HeLa cells without transfection of plasmids. HeLa cells were immunostained with the anti-SRB-RGS antibody or PBS containing preimmune serum and then fluorescein-5-isothiocyanate (FITC)-conjugated anti-rabbit immunoglobulin (green fluorescence) as a secondary antibody and observed on a confocal laser-scanning microscopy after staining of the nucleus with PI (red fluorescence). SRB-RGS was stained in the cytoplasm and in the nucleus stained with PI in HeLa cells (Fig. 3C). These observations showed that intrinsic SRB-RGS localized in the cytoplasm and the nucleus, but not in the plasma membrane. In some cells, the cytoplasm was immunostained, but the nucleus was not. SRB-RGS may be localized in either the nucleus or the cytoplasm of the cell and shuttle between the nucleus and the cytoplasm under some condition. These findings by intrinsic SRB-RGS (Fig. 3C) were consistent with the observations in the HeLa cell or the COS-7 cells transfected with pEGFPSRB-RGS (Figs. 3A, B).

The whole cell lysate from HeLa cells without transfection with pcDNASRB-RGS was analyzed by Western blotting using the anti-SRB-RGS antibody and then peroxidase linked anti-rabbit IgG. Consequently, an apparent band with the mobility corresponding to SRB-RGS was detected (Fig. 3D, a white arrow). The band of SRB-RGS was observed in the whole cell lysate from COS-7 cells without transfection of pcDNASRB-RGS as well (data not shown).

These findings (Figs. 3C, D and Fig. 1C) showed that the intrinsic SRB-RGS was expressed in the cells. The putative SRB-RGS deduced from cDNA sequence [18] was identified.

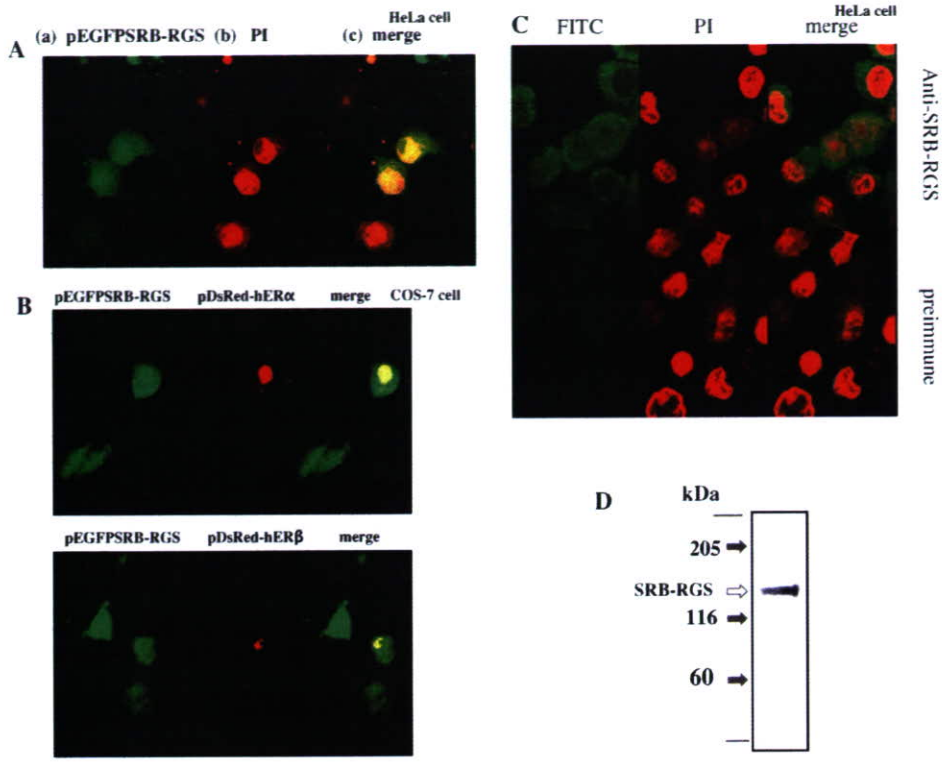

Fig. 3. Subcellular Localization and Identification of SRB-RGS

(A, B) Subcellular localization of EGFP-tagged SRB-RGS. The HeLa cells (A) or COS-7 cells (B) were transiently transfected with pEGFPSRB-RGS (A: 0.2 μg, B: 2 μg) with (B) or without (A) pDsRed-hERα (2 μg) or pDsRed-hERβ (2 μg). Fluorescence was observed by a confocal laser-scanning microscopy after (A) or without (B) staining of the nucleus with PI. (C) Immunostainning of intrinsic SRB-RGS. HeLa cells without transfection of any plasmids were stained with the anti-SRB-RGS antibody or PBS containing preimmune serum and then fluorescein-5-isothiocyanate (FITC)-conjugated anti-rabbit immunoglobulin (green fluorescence). They were viewed on a confocal laser-scanning microscopy after PI staining of the nucleus (red fluorescence). (A—C) The same microscopic field of the cells was shown in Green fluorescence (SRB-RGS), Red fluorescence (nucleus) and merge. (D) Identification of intrinsic SRB-RGS by Western blotting. The HeLa cells without transfection of pcDNASRB-RGS were lysed in the solubilization buffer as mentioned in Materials and Methods. The lysate was subjected on 7% SDS-PAGE and transferred to a nitrocellulose membrane. The membrane was incubated with the anti-SRB-RGS antibody and then peroxidase-linked anti-rabbit IgG. The band on the membrane was visualized as the chemiluminescent signal by development of the peroxidase activity.

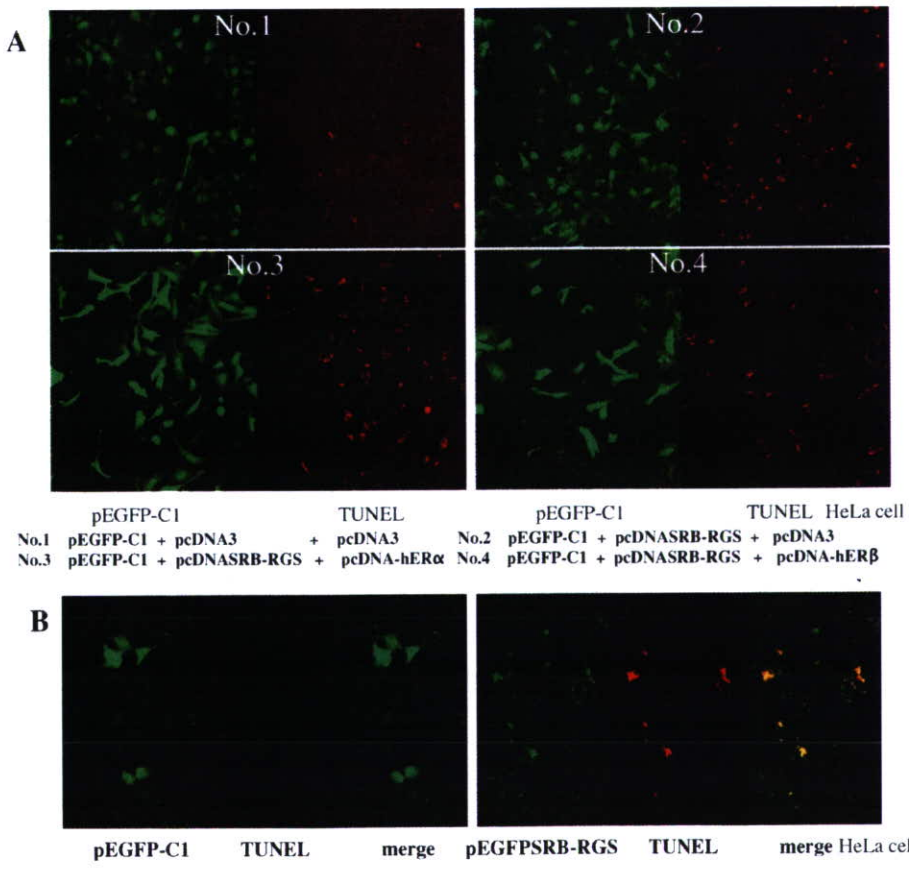

Fig. 4. The Cell Death in HeLa Cells Induced by SRB-RGS

The HeLa cells were grown on glass cover slips and transiently transfected with the plasmids. (A) No. 1 pcDNA3 (3 μg)+pcDNA3 (3 μg), No. 2 pcDNASRB-RGS (3 μg)+pcDNA3 (3 μg), No. 3 pcDNASRB-RGS (3 μg)+pcDNA-hERα (3 μg) and No. 4 pcDNASRB-RGS (3 μg)+pcDNA-hERβ (3 μg) were individually cotransfected with pEGFP-C1 (3 μg) to normalize the transfection efficiency to HeLa cells. (B) HeLa cells were transfected with pEGFP-C1 (3 μg) or pEGFPSRB-RGS (3 μg). The TUNEL assay was performed on the cells to assess DNA fragmentation, as mentioned in Materials and Methods, and the cells were viewed on a confocal laser-scanning microscopy. Red fluorescence: staining by TUNEL assay. pEGFP-C1: the empty plasmid of pEGFPSRB-RGS. pcDNA3: the empty plasmid of pcDNASRB-RGS, pcDNA-hERα and pcDNA-hERβ.

A blast search of SRB-RGS on a mouse genome database of National Center for Biotechnology Information (NCBI) (U.S.A.) revealed that SRB-RGS gene locates on a mouse chromosome 5, splitting into some exons. SRB-RGS gene actually locates on a rat, mouse and human chromosomes according to the genome databases, supporting strongly the identification of intrinsic SRB-RGS in the cells.

Induction of the Cell Death in HeLa Cells by Overexpression of SRB-RGS Overexpression of SRB-RGS in HeLa cells induced the appearances of cell shrinkage and nuclear fragmentation (apoptotic appearances). We examined whether the shrinked cells were TUNEL-positive. As indicated at the bottom of Fig. 4A, No. 1: pcDNA3 (3 μg)+pcDNA3 (3 μg), No. 2: pcDNASRB-RGS (3 μg)+pcDNA3 (3 μg), No. 3: pcDNASRB-RGS (3 μg)+pcDNA-hERα (3 μg), and No. 4: pcDNASRB-RGS (3 μg)+pcDNA-hERβ (3 μg) were individually cotransfected with pEGFP-C1 (3 μg) to normalize the transfection efficiency to HeLa cells. Consequently, the ratios of the TUNEL-positive cells in the cells transfected with pcDNASRB-RGS to the control (No. 1) increased to 4.9-, 3.4- and 4.4-fold (Nos. 2, 3 and 4, respectively) (the ratios of means in two microscopic fields normalized by the transfection efficiency) (Fig. 4A). By transfection of pcDNA3 (3 μg) or pcDNASRB-RGS (3 μg), 3.4 or 16.0%, respectively, of the total HeLa cells were TUNEL-positive (data not shown). Introduction of ERs did not significantly change the ratio of the cell death. The cell death was ERs-independent. To examine further whether overexpression of SRB-RGS caused cell death in the cells, HeLa cells were transfected with pEGFPC-1 or pEGFPSRB-RGS in the absence or presence of Z-VAD-FMK (the caspases inhibitor), and a TUNEL assay was performed. The cells which overexpressed EGFP (the green fluorescent cells) were TUNEL-negative, whereas almost all cells which overexpressed EGFP-tagged SRB-RGS (the green fluorescent cells) were TUNEL-positive (red fluorescence) (Fig. 4B), showing the introduction of SRB-RGS to the cells induced the cell death. The ratio of TUNEL-positive cells did not decrease in HeLa cells which overexpressed EGFP-tagged SRB-RGS in the presence of Z-VAD-FMK (data not shown). The cell death induced by SRB-RGS was caspases-independent.

The significant apoptotic appearance such as cell shrinkage and nuclear fragmentation was not observed by overexpression of SRB-RGS in COS-7 cells. pcDNASRB-RGS (or pcDNA3) (0.2 μg or 3 μg) was cotransfected with pEGFP-C1 (3 μg) to COS-7 cells. The ratios of the TUNEL-positive cells did not increased by overexpression of SRB-RGS (data not shown), suggesting that the suppression effects of SRB-RGS overexpression on the ERα-, ERβ- and ERα+ERβ-mediated transcriptional activities in COS-7 cells (Fig. 2) were not due to the cell death of the COS-7 cells.

DISCUSSION

We attempted to characterize the physiological functions of SRB-RGS in this paper. Our studies provide evidence that SRB-RGS bound to ERs *in vitro* and in the nuclei of the cells (Figs. 1A, B) even when ERs bind to DNA (Fig. 1C), and suppressed the ERs-mediated transcription activities (Fig. 2). SRB-RGS induced the cell death in the HeLa cells ERs- and caspase-independently (Fig. 4). In addition, SRB-RGS was localized in nucleus and cytoplasm, and identified in HeLa cells (Fig. 3).

SRB-RGS and ERs were coimmunoprecipitated by the anti-SRB-RGS antibody, anti-hERα antibody or anti-hERβ antibody. Full-length SRB-RGS interacted with full-length ERs even in the absence of estradiol *in vitro* (Fig. 1A). SRB-RGS 1-495 a.a. and full-length rERα interacted in either the absence or presence of estradiol in a yeast two-hybrid system (Table 1). Full-length hERα interacted with full-length SRB-RGS in the COS-7 cells in either the absence or presence of estradiol in a mammalian two-hybrid system as well (Fig. 1B). These findings suggested that estradiol was not a trigger of interaction between SRB-RGS and ERs. They may interact constitutively, or some unknown trigger may be necessary for the interaction. Full-length SRB-RGS hardly interacted with rERα in yeast cells (Table 1). SRB-RGS and ERs prepared in mammalian systems (an *in vitro* transcription translation system, a mammalian two-hybrid system, the nuclear extract from the rat uterus) could interact with each other (Figs. 1A, B, C). The chemical modification of SRB-RGS and/or ERs, such as phosphorylation, may be a trigger for the interaction *in vivo*. In fact, SRB-RGS has the many phosphorylation sites in the NH_2-terminal region (the ER-binding region).[18] The transcriptional activities of estrogen receptors might be enhanced after dissociation of chemically modified SRB-RGS.

We introduced the smallest and still effective amount of pcDNASRB-RGS to suppress the ERs-mediated transcriptional activities to the cells. In this condition, the CMV promoter-driven transcriptional activity (pcDNAβ-gal) was not suppressed (data not shown). This finding and the results of quantitative real time RT-PCR of the expression of hERα (or hERβ) mRNA (mentioned above) showed that introduction of pcDNASRB-RGS did not affect the ERs expression driven by CMV promoter (pcDNA-hERα or pcDNA-hERβ), suggesting the suppression effects were not due to decrease of ERs expression in the cells. SRB-RGS was localized in the nucleus (Fig. 3), bound to hERα in the nucleus of the cell (Fig. 1B), and interacted with ERs bound to DNA (estrogen response element) (Fig. 1C). SRB-RGS may suppress the ER-mediated transcriptional activities through the interaction with ERs bound to DNA (Fig. 2). SRB-RGS might affect the signal transduction of the membrane-associated receptors in the cytoplasm. Proteins with both PDZ and RGS domains were reported, such as RGS12[25] and PDZ-RGS3.[26] SRB-RGS was the first protein among them to report the suppression of the transcriptional activities.

Recently, it was shown that the nucleotide sequence of SRB-RGS (DDBJ/GenBank/EMBL Accession AB055153) is identical with that of the newly isolated full-length rRGS3 cDNA (NCBI secondary DNA database Accession NM019340). Previous partial hRGS3 (1-519 a.a., corresponding to SRB-RGS 399-967 a.a.) was localized in the cytoplasm, whereas the truncated variant of previous partial hRGS3 termed hRGS3T (previous hRGS3 314-519 a.a., corresponding to SRB-RGS 763-967 a.a.) was found predominantly in the nucleus and partially in the plasma membrane.[27] SRB-RGS could enter the nucleus without ERs (Fig. 3). In fact, previous partial hRGS3 and hRGS3T have the nuclear localization signal (NLS) sequences.

Overexpression of hRGS3T, but not previous hRGS3, followed by serum deprivation resulted in apoptosis of CHO cells.[27] Overexpression of SRB-RGS induced the cell death in HeLa cells without serum deprivation (Fig. 4). SRB-RGS might induce the cell death through caspases-independent affection to survival signals of the cell.

Acknowledgements This study was supported in part by Research Project Grants (Nos. 14-112, 15-104A, 16-105M) from Kawasaki Medical School. We thank Yasue Miyasako, Hiroko Yamamoto, Akane Tsubouti, Tomoko Takada, Mayu Asahi, Marie Sugimoto, Masako Jinbo, Masako Matsuura, Kumiko Ohchi, Yohsuke Utihi (Department of Clinical Engineering, Kawasaki College of Allied Health Professions) for their technical assistance. We also thank Dr. Yoshinobu Tone (Department of Biochemistry, Kawasaki Medical School) for his helpful advices.

REFERENCES

1) Green S., Chambon P., *Trends Genet.*, **4**, 309—314 (1988).
2) Ikeda M., Ogata F., Curtis S. W., Lubahn D. B., French F. S., Wilson E. M., Korach K. S., *J. Biol. Chem.*, **268**, 10296—10302 (1993).
3) Mangelsdorf D. J., Thummel C., Beato M., Herrlich P., Schutz G., Umesono K., Blumberg B., Kastner P., Mark M., Chambon P., Evans R. M., *Cell*, **83**, 835—839 (1995).
4) Onate S. A., Tsai S. Y., Tsai M.-J., O'Malley B. M., *Science*, **270**, 1354—1357 (1995).
5) Ogryzko V. V., Schiltz R. L., Russanova V., Howard B. H., Nakatani Y., *Cell*, **87**, 953—959 (1996).
6) Bannister A. J., Kouzarides T., *Nature* (London), **384**, 641—643 (1996).
7) Yeh S., Chang C., *Proc. Natl. Acad. Sci. U.S.A.*, **93**, 5517—5521 (1996).
8) Fondell J. D., Ge H., Roeder R. G., *Proc. Natl. Acad. Sci. U.S.A.*, **93**, 8392—8333 (1996).
9) Freedman L. P., *Cell*, **97**, 5—8 (1999).
10) Nagy L., Kao H.-Y., Chakravarti D., Lin R. J., Hassing C. A., Ayer D. E., Schreiber S. L., Evans R. M., *Cell*, **89**, 373—380 (1997).
11) Heinzel T., Lavinsky R. M., Mullen T.-M., Soderstrom M., Laherty C. D., Torchia J., Yang W.-M., Brard G., Ngo S. D., Davie J. R., Seto E., Eisenman R. E., Rse D. W., Glass C. K., Rosenfeld M. G., *Nature* (London), **387**, 43—48 (1997).
12) Alland L., Muhle R., Hou H., Jr., Potes J., Chin L., Schreiber-Agus N., DePinho R. A., *Nature* (London), **387**, 49—55 (1997).
13) McKenna N. J., O'Malley B. W., *Cell*, **108**, 465—474 (2002).
14) Narlikar G. J., Fan H.-T., Robert E., Kingston R. E., *Cell*, **108**, 475—487 (2002).
15) Siderovski D. P., Strockbine B., Behe C. I., *Crit. Rev. Biochem. Mol. Biol.*, **34**, 215—251 (1999).
16) Linare J.-L., Wendling C., Tomasetto C., Rio M.-C., *FEBS Lett.*, **480**, 249—254 (2000).
17) Hata Y., Nakanishi H., Takai Y., *Neurosci. Res.*, **32**, 1—7 (1998).
18) Ikeda M., Hirokawa M., Satani N., Kinoshita T., Watanabe Y., Inoue H., Tone S., Ishikawa T., Minatogawa Y., *Gene*, **273**, 207—214 (2001).
19) Ogawa S., Inoue S., Watanabe T., Hiroi H., Orimo A., Hosoi T., Ouchi Y., Muramatsu M., *Biochem. Biophys. Res. Commun.*, **243**, 122—126 (1998).
20) Ikeda M., Okai M., Miyoshi T., Minatogawa Y., *Horm. Metab. Res.*, **34**, 425—430 (2002).
21) Wang H., Peter G., Xeng X., Tang M., Ip W., Khan S., *J. Biol. Chem.*, **270**, 23322—23329 (1995).
22) Chaidarun S. S., Swearingen B., Alexander J. M., *J. Clin. Endocrinol. Metab.*, **83**, 3308—3315 (1998).
23) Kuiper G. G., Carlsson B., Grandien K., Enmark E., Haggblad J., Nilsson S., Gustafsson J.-Å., *Endocrinology*, **138**, 863—870 (1997).
24) Lindberg M. K., Monverare S., Skrtic S., Gao H., Dahlman-Wright K., Gustafsson J.-Å., Ohlsson C., *Mol. Endocrinol.*, **17**, 203—208 (2003).
25) Snow B. E., Antonio L., Suggs S., Gutstein H. B., Siderovski D. P., *Biochem. Biophys. Res. Commun.*, **233**, 770—777 (1997).
26) Lu Q., Sun E. E., Klein R. S., Flanagan J. G., *Cell*, **105**, 69—79 (2001).
27) Dulin N. O., Pratt P., Tiruppathi C., Niu J., Voyno-Yasenetkaya T., Dunn M. J., *J. Biol. Chem.*, **275**, 21317—21323 (2000).

Nuclear cyclin B1 in human breast carcinoma as a potent prognostic factor

Takashi Suzuki,[1,5] Tomohiro Urano,[3] Yasuhiro Miki,[1] Takuya Moriya,[1] Jun-ichi Akahira,[1] Takanori Ishida,[2] Kuniko Horie,[4] Satoshi Inoue[3,4] and Hironobu Sasano[1]

Departments of [1]Pathology and [2]Surgery, Tohoku University School of Medicine, 2-1 Seiryo-machi, Aoba-ku, Sendai, Miyagi-ken, 980-8575; [3]Department of Geriatric Medicine, Graduate School of Medicine, The University of Tokyo, 7-3-1 Hongo, Bunkyo-ku, Tokyo, 113-8655; [4]Research Center for Genomic Medicine, Saitama Medical University, 1397-1 Yamane, Hidaka, Saitama, 350-1241, Japan

(Received November 30, 2006/Revised December 14, 2006/Accepted December 24, 2006/Online publication March 16, 2007)

Cyclin B1 is translocated to the nucleus from the cytoplasm, and plays an essential role in cell proliferation through promotion of mitosis. Although overexpression of cyclin B1 was previously reported in breast carcinomas, the biological significance of the intracellular localization of cyclin B1 remains unclear. Therefore, in this study, we examined cyclin B1 immunoreactivity in 109 breast carcinomas, according to the intracellular localization, that is, nucleus, cytoplasm or total (nucleus or cytoplasm). Total cyclin B1 was detected in carcinoma cells in 42% of breast carcinomas examined, whereas nuclear and cytoplasmic cyclin B1 were positive in 17 and 35% of the cases, respectively. Total or cytoplasmic cyclin B1 were positively associated with histological grade, mitosis, Ki-67, p53, c-myc or 14-3-3σ, and inversely correlated with estrogen or progesterone receptor. Nuclear cyclin B1 was significantly associated with tumor size, lymph node metastasis, histological grade, mitosis, Ki-67 or polo-like kinase 1. Only nuclear cyclin B1 was significantly associated with adverse clinical outcome of the patients, and multivariate analyses of disease-free and overall survival demonstrated nuclear cyclin B1 as the independent marker. A similar tendency was detected in the patients receiving adjuvant therapy after surgery. These results suggest that an onocogenic role of overexpressed cyclin B1 is mainly mediated in nuclei of breast carcinoma cells, and the nuclear translocation is regulated by polo-like kinase 1 and 14-3-3σ. Nuclear cyclin B1-positive breast carcinoma is resistant to adjuvant therapy, and nuclear cyclin B1 immunoreactivity is a potent prognostic factor in breast carcinoma patients. (*Cancer Sci* 2007; 98: 644–651)

Breast cancer is one of the most common malignancies in women worldwide. Invasive breast cancer has been generally regarded as a disease that metastasizes in an early phase, and clinical outcome of breast carcinoma patients is markedly influenced not only by metastasis of the tumor but also by proliferation activity of the tumor.[1] In fact, a multitude of prognostic factors identified for breast cancer have been demonstrated to be directly or indirectly related to proliferation of breast carcinoma cells.

It is well-known that proliferation of carcinoma cells is closely associated with altered regulation of the cell cycle.[2] Cell cycle progression is mediated by activation of a highly conserved family of cyclin-dependent kinases (Cdk),[3] and activation of a Cdk requires binding to a specific regulatory subunit, named a cyclin. Among the cyclins, cyclin B1 plays an essential role as a mitotic cyclin in the entry of mitosis from G_2 phase.[4] Overexpression of cyclin B1 has been reported in various human tumors, and some of these studies demonstrated the clinical significance of cyclin B1 as a poor prognostic factor for some cancers,[5–7] including lymph node-negative breast carcinoma.[8]

Cyclin B1 is initially localized in the cytoplasm, and is translocated to the nucleus at the beginning of mitosis.[9] Nuclear translocation of cyclin B1 is considered very important to facilitate access of the cyclin B–Cdc2 (also named Cdk1) complex to its nuclear substrate and promote mitosis.[4] Therefore, it becomes very important to examine the intracellular localization of cyclin B1 in tumor tissues, in order to obtain a better understanding of the biological roles of cyclin B1.[10] Previously, Winters *et al.* reported that nuclear cyclin B1 immunoreactivity was significantly associated with reduced disease-free survival of breast carcinoma patients in a log-rank analysis.[11] However, no other information is available regarding the intracellular localization of cyclin B1 in breast carcinoma tissue, and the biological significance of cyclin B1 remains unclear at this juncture. Therefore, in the present study, we examined the intracellular immunolocalization of cyclin B1, and correlated these findings with various clinicopathological parameters of the patients, including their clinical outcome.

Materials and Methods

Patients and tissues. One hundred and nine specimens of invasive ductal carcinoma of the breast were obtained from female patients who underwent mastectomy from 1984 to 1987 at the Department of Surgery, Tohoku University Hospital, Sendai, Japan. Breast tissue specimens were obtained from patients with a mean age of 53.1 years (range 23–82 years). The patients did not receive chemotherapy, irradiation or hormonal therapy prior to surgery. Review of the charts revealed that 85 patients received adjuvant chemotherapy (mitomycin C, methotrexate and fluorouracil, $n = 80$; cyclophosphamide, doxorubicin and fluorouracil, $n = 3$; and cyclophosphamide, mitomycin C and fluorouracil, $n = 2$). Seventeen patients received radiation therapy, and 12 patients received tamoxifen therapy after the surgery. The mean follow-up time was 106 months (range 4–157 months). The histological grade and tubule formation of each specimen was evaluated according to the method of Elston and Ellis.[12] All specimens were fixed with 10% formalin and embedded in paraffin wax. Research protocols for this study were approved by the Ethics Committee at both Tohoku University School of Medicine.

Antibodies. A rabbit polyclonal antibody for cyclin B1 (H-433 [sc-752]) was purchased from Santa Cruz Biotechnology (Santa Cruz, CA, USA). This antibody was raised against a recombinant peptide corresponding to amino acids 1–433 representing full-length human cyclin B1. Monoclonal antibodies for estrogen receptor α (ER; ER1D5), progesterone receptor (PR; MAB429), Ki-67 (MIB1), p53 (DO7) and c-myc (1-6E10) were purchased from Immunotech (Marseille, France), Chemicon (Temecula, CA, USA), DAKO (Carpinteria, CA, USA), Novocastra Laboratories (Newcastle, UK) and Cambridge Research Biochemical (Cambridge, UK), respectively. Rabbit polyclonal antibodies for HER2 (A0485) and polo-like kinase 1 (PLK1; 06-813) were obtained

[5]To whom correspondence should be addressed.
E-mail: t-suzuki@patholo2.med.tohoku.ac.jp

doi: 10.1111/j.1349-7006.2007.00444.x